Journal of Applied Geophysics xxx (2010) xxx–xxx

Contents lists available at ScienceDirect

Journal of Applied Geophysics

journal homepage: www.elsevier.com/locate/jappgeo

The contribution of geophysical techniques to site characterisation and liquefaction risk assessment: Case study of Nafplion City, Greece

V.K. Karastathis [a,*], P. Karmis [b], T. Novikova [a], Z. Roumelioti [c], E. Gerolymatou [a], D. Papanastassiou [a], S. Liakopoulos [a], P. Tsombos [b], G.A. Papadopoulos [a]

[a] National Observatory of Athens, Institute of Geodynamics, PO Box 20048, GR 118 10 Athens, Greece
[b] Institute of Geology and Mineral Exploration (IGME),), S. Loui 1, 3rd Entrance Olympic Village, Acharnae 136 77, Greece
[c] Department of Geophysics, Aristotle University of Thessaloniki, P.O. Box 352-1, 54124 Thessaloniki, Greece

ARTICLE INFO

Article history:
Received 10 June 2009
Accepted 18 September 2010
Available online xxxx

Keywords:
Liquefaction
Shallow seismic reflection
Microzonation study
Nafplion
Depth migration

ABSTRACT

We present an example of how geophysical methodologies can considerably contribute to seismic and liquefaction risk assessment in an area where urban development is planned.
The inspection for possible hidden faults by geophysical methods is particularly critical, since such a possibility could practically hinder the town planning in this area. However, even if no primary threats exist within the area, the response of the foundation soil to various scenarios of historical earthquakes, which have affected the place in the past, must be examined. The geophysical methodologies could also assist this analysis, contributing with the calculation of the amplification of the seismic motion from the bedrock up to the surface.
The investigation area of Nafplion, Greece, was suspected to have high liquefaction potential since the foundation soil consists of loose sandy silt with a very shallow aquifer.
The implementation of gravity and seismic methods considerably aided the investigation for possible seismic faults. Special emphasis was given to seismic depth migration and particularly to the construction of valid velocity models, in order to precisely calculate the dip characteristics of the structures.
Shallow seismic techniques were also applied to provide the near-surface velocity structure, which is a prerequisite for assessing the liquefaction risk. In particular, our case study provides an example of how seismic methods (seismic reflection, seismic refraction, seismic modelling, MASW, multichannel analysis of microtremors and crosshole investigations) when combined with geotechnical borehole testing, enhance the reliability of their output and allow the coverage of wide areas in a cost-effective way in comparison to standard borehole tests. Data and information provided by the application of the geophysical methods were subsequently incorporated in the liquefaction risk assessment at several selected sites within the study area. Factors of safety against liquefaction and liquefaction potential values were computed for three scenario earthquakes that were selected on the basis of the known seismic impact of past earthquakes in the town of Nafplion. We found that liquefaction probability can reach values as high as 80% at some sites depending on the selected earthquake scenario. The formations most prone to liquefaction are detected at depths between 5 and 10 m. This information can be helpful for making risk-based design decision in this region.

1. Introduction

The urban planning of many cities is usually based on economic and social factors, without taking into account the local geology and the active geodynamic processes. This fact combined with the continuous increase of the population and the industrialization in these suburban areas, explains the dramatic increase of the seismic impact during the last decades. Nafplion, NE Peloponnese, Greece (Fig. 1), is one of those cities originally founded on safe ground, but expanding in recent years along the coastline on ground of questionable safety factor with reference to seismic and liquefaction risk.

The present paper mainly aims to show how the geophysical investigations can play a significant role in a characterisation study of the foundation soil in an area that is intended for urban development. Their application can accelerate the study and easily spread out the results to wider areas. Although the paper is mainly focused on the analysis and the evaluation of the geophysical results, reference is also given to their incorporation in techniques for the seismic and liquefaction risk assessment, in order to provide an integrated picture of the contribution of the geophysical surveys in the whole procedure.

According to the legal framework of many countries, regular building is restricted in areas adjacent to active faults. Similar

* Corresponding author. Fax: +30 210 3490180.
E-mail address: Karastathis@gein.noa.gr (V.K. Karastathis).

0926-9851/$ – see front matter © 2010 Elsevier B.V. All rights reserved.
doi:10.1016/j.jappgeo.2010.09.003

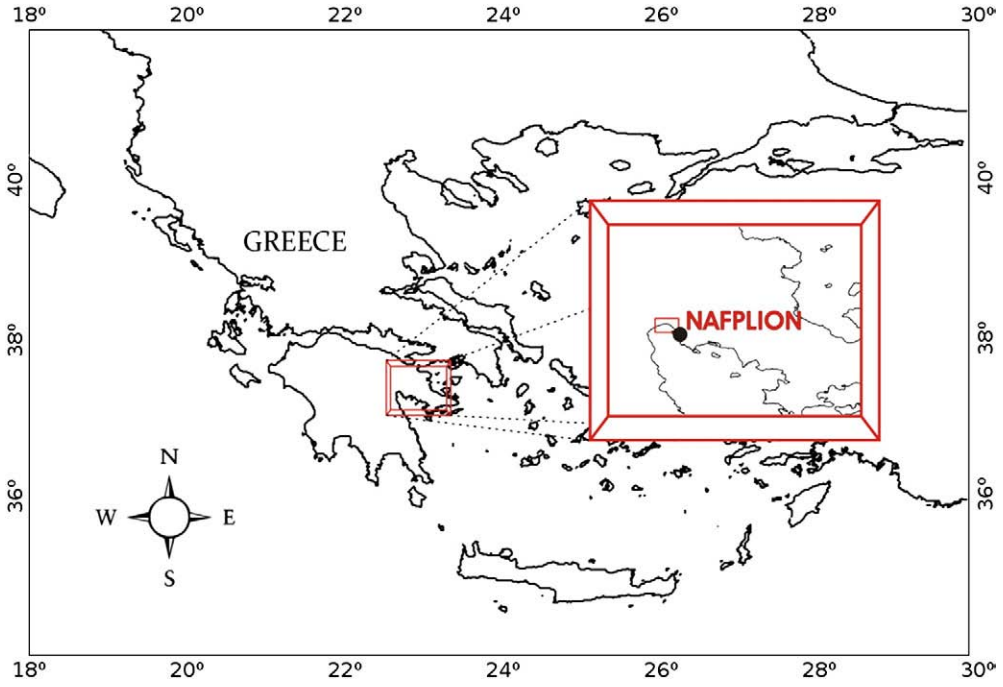

Fig. 1. Location map of the survey area (small box) close to Nafplion City.

restrictions apply to soils susceptible to liquefaction due to strong earthquakes, to areas with slope stability problems, to unconsolidated embankments, etc. (Greek Earthquake Resistant Design Code, 2000). Therefore, building can be allowed only if these factors are excluded. However exceptions are also possible, in special cases, after conducting special studies on the assessment and encountering with these particular risks.

In the case of Nafplion we mainly focused on the investigation of active faults within the study area by the implementation of gravity and seismic techniques. Information derived from the near-surface seismic measurements was later incorporated into the analysis of the liquefaction risk at specific sites, since evidence was found for susceptibility to soil liquefaction.

2. Methodology

The geophysical techniques aided the investigation of active faults as possible earthquake sources in the study area. The gravity survey, as a reconnaissance method, was suitable for locating possible deformation of the bedrock, which could be attributed to faults. As a follow-up survey, seismic depth imaging delineated the detected suspicious structures and finally defined if these could be related to active faults.

The geophysical methods contributed also to the liquefaction risk assessment by providing the near-surface velocity structure needed for the calculation of the amplification of the strong seismic motion from the bedrock up to the surface. The liquefaction risk assessment was performed by a fully nonlinear, effective stress based ground response analysis.

Since accelerographic data from strong earthquakes were not available for the investigation area (Theodulidis et al., 2004), our analysis of the liquefaction potential was based on synthetic data. Peak Ground Acceleration (PGA) values required for the computation of the Factor of Safety against liquefaction were computed by a finite-fault stochastic strong ground motion simulation described in detail by Beresnev and Atkinson (1997, 1998). Synthetic strong ground motion records were computed for different earthquake scenarios. The reliability of the liquefaction risk assessment greatly depends upon good knowledge of the potential earthquake sources that could affect the sites of interest. Archives of historical seismicity may provide some relevant information but they usually suffer from uncertainty and incompleteness. Instrumental earthquake records surely are more accurate and complete and, therefore, more reliable for seismic source characterization. On the other hand, instrumental seismicity in Greece covers only the last about 100 years, a time length which is exceeded by several times by the mean repeat time of strong earthquakes. Therefore, in our case, the simulation of significant historical earthquakes that affected the study region was judged as the best approximation to get the expected accelerogram at the level of bedrock. It must be noted, however, that within the frame of the present work we do not examine the possibility for the repetition of these historical earthquakes.

Using the synthetic acceleration data and the knowledge of the near-surface seismic velocity structure, we finally calculated the acceleration up to the surface in order to study the susceptibility of the soil to liquefaction. In particular, the seismic methods provided the estimation of the shear seismic velocity for the top 30 m of the foundation ground. Although it was possible to have this information for deeper layers, normally there was no need, since at these depths the confining pressure was high enough to counter the pore pressure.

A diagram presenting the steps of this methodology and how geophysical techniques are contributing to the liquefaction risk assessment is shown in Fig. 2.

Geophysical methods have been applied in the past to provide information for both seismic hazard and liquefaction risk assessment (Benjumea et al., 2003; Yilmaz et al., 2006; Hayashi et al., 2006; Yoon and Rix, 2007); however, engineers like to see a great number of successful case-studies in order to adopt this kind of surveys among the standard techniques.

3. Geological setting and past seismicity

The regional geology of the Argos plain is composed of coastal deposits of loose, fine silty sands and silty–clayey soils, fluviotorrential deposits and alluvial fans. The underlying bedrock includes Alpine and post-Alpine sediments, such as flysch, limestone and Neogene marl conglomerates. In particular, the area of investigation (see Fig. 3) is formed by alluvial, mainly lagoonal deposits, overlying flysch and limestone formations.

Please cite this article as: Karastathis, V.K., et al., The contribution of geophysical techniques to site characterisation and liquefaction risk assessment: Case study of Nafplion City,..., J. Appl. Geophys. (2010), doi:10.1016/j.jappgeo.2010.09.003

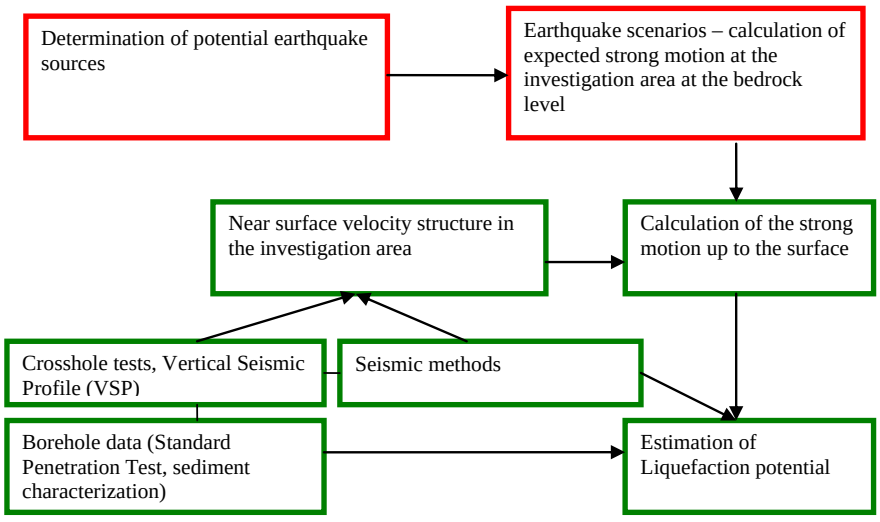

Fig. 2. The geophysical methods have a key role in the methodology of the seismic and liquefaction risk assessment.

In some geological maps, faults have been mapped bounding the steep limestone cliffs south and east of the Nafplion area. These faults are most likely inactive, as they have no geomorphological evidence of tectonic activity. To the south of Nafplion, at the base of the limestone mass and at elevation of a few meters above the present sea level, uplifted beaches are observed. These beaches contain characteristic fossil (Strobus Bubonious fauna) indicating that they are associated to the sea level highstand of 5e of the interglacial Oxygen Isotope stages (Dufaure, 1977), which correspond to date of about 120 ka. Beaches of this age and with same elevations also exist in other regions of Greece characterised by very low tectonic activity. This further supports the suggestion that the faults that bound the limestone hills to the south of the study area very likely have been inactive at least for the last hundred thousand years.

With regard to the groundwater regime within the Quaternary deposits, successive groundwater aquifers are developed, being under intensive exploitation by well boring. This has resulted in considerable seawater intrusion in recent years. Within some parts of the investigation area, at an altitude of a few meters above sea level, a weak unconfined coastal aquifer is developed at a small depth near the surface, which is underlain by deeper confined aquifers. This shallow unconfined aquifer is associated with a local marshland. The sandy–silty, clayey–silty nature of soils and the presence of the groundwater table near the surface constitute a particularly unfavourable regime for the construction of building foundations. Within this regime an attentive assessment of the liquefaction potential is required.

In historical seismicity archives of the broader area where Nafplion is situated, liquefaction has been reported in association with the 2 June 1898, $M = 7.2$, earthquake with its epicentre (37.6°N, 22.5°E) located only 27 km to the NWW of Nafplion (Ambraseys and Jackson, 1990; Papadopoulos and Lefkopoulos, 1993; Papathanassiou et al., 2005). Evaluation of macroseismic observations concluded that the earthquake was of intermediate focal depth (Papazachos and

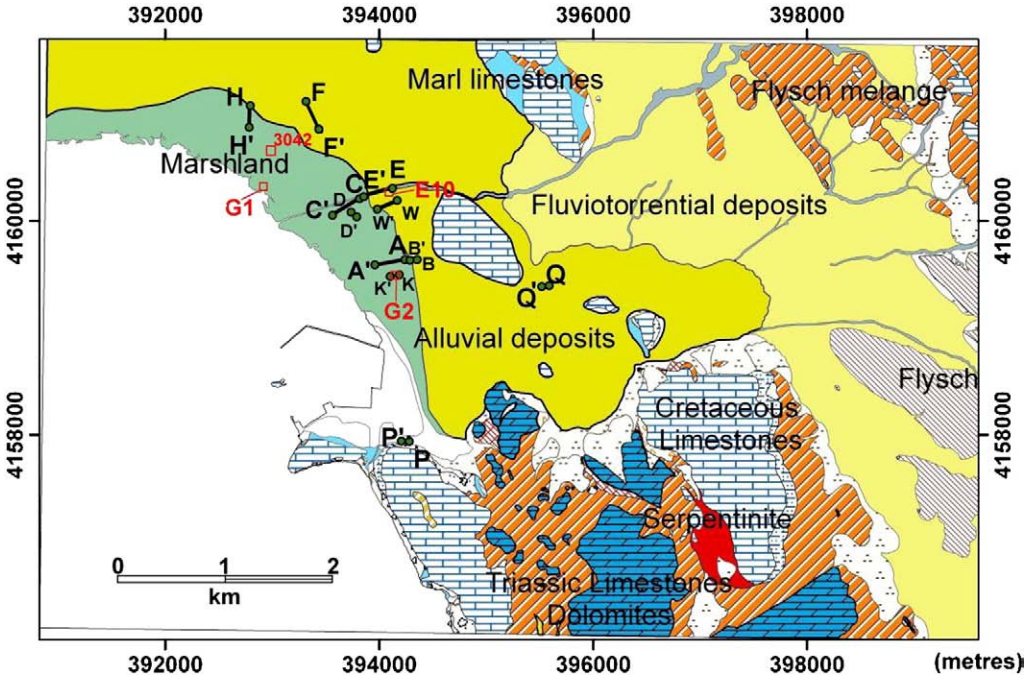

Fig. 3. Geological map of the investigated area (Fotiadis A. and Mitropoulos D., IGME internal report, 2008). The seismic lines are presented in black colour. The coordinates are referred to the Greek Geodetic Reference System (GGRS-87).

Please cite this article as: Karastathis, V.K., et al., The contribution of geophysical techniques to site characterisation and liquefaction risk assessment: Case study of Nafplion City,..., J. Appl. Geophys. (2010), doi:10.1016/j.jappgeo.2010.09.003

Papazachou, 2003). However, other shallow earthquakes of significant magnitude, from three known major faulted zones (see Fig. 4), have also affected the building environment of the town of Nafplion during historical times (Papazachos and Papazachou, 2003). These zones are:

- Iria fault ("Argos" fault in Papazachos and Papazachou, 2003)
- The fault of Epidaurus and
- The fault of Xylokastro, at the south coast of Corinthiakos gulf.

4. Geophysical investigations

Geophysical techniques were carried out with the aim to detect possible seismic faults within the study area, as well as to determine near-surface velocity models in order to contribute to the estimation of the soil amplification of the expected seismic ground motion and the liquefaction risk assessment.

4.1. Geophysical investigations for mapping the bedrock relief and detection of possible faults

Firstly, we performed a gravity survey, as a reconnaissance method, suitable for locating possible deformation of the bedrock that could be attributed to faults. Interesting features revealed by this first survey were further studied by seismic depth imaging to delineate their characteristics and investigate whether they could be related to active faults.

4.1.1. Gravity survey

The aim of the gravity survey was to derive quantitative information regarding the geological structure of the area and more specifically its main tectonic elements. A network of 270 gravity stations was established in the area, distributed in such a way that the mean distance between any two neighbouring stations was approximately 350 m.

The survey involved simultaneous gravity and GPS observations. Gravity measurements were obtained using a new generation electronic gravity-meter with resolution of 1 μGal. Precise coordinates of the gravity stations were assigned by differential positioning using two geodetic GPS stations. The coordinates were referred to the Greek Geodetic Reference System (GGRS-87).

To define the necessary topographic corrections, a Digital Elevation Model (DEM) was compiled, based on high resolution digital topographic data issued by the Hellenic Army Geographical Survey (HAGS). The terrain correction was calculated for an area of radius 21 km around each station. Each area was divided in three co-central "ring" zones with outer radii of 50 m, 1500 m and 21 km, respectively. For the near-field terrain effects (inner zone of radius of

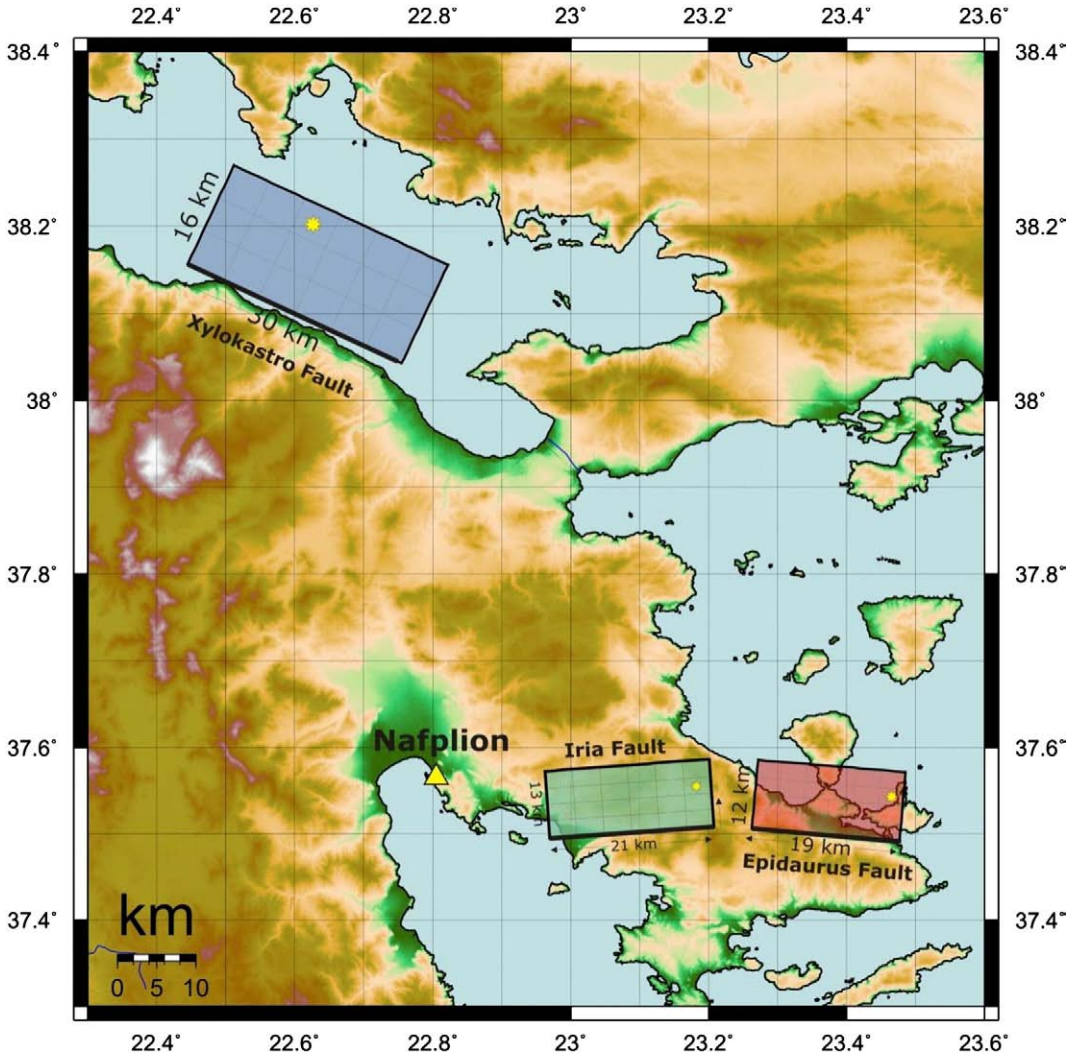

Fig. 4. Three faulted zones, which have been associated with strong historical earthquakes that affected the structures of the city. The rectangular boxes present the surface projection of the three scenario earthquake sources (thicker side of each rectangular corresponds to the surface trace of the fault). In the applied method, the seismic sources are treated as simple rectangular surfaces with dimensions determined from empirical relations. The asterisk on each surface denotes the rupture initiation point.

Please cite this article as: Karastathis, V.K., et al., The contribution of geophysical techniques to site characterisation and liquefaction risk assessment: Case study of Nafplion City,..., J. Appl. Geophys. (2010), doi:10.1016/j.jappgeo.2010.09.003

50 m) a Hammer zone chart was used. The correction for the intermediate (50 m–1500 m) and outer (1.5 km–21 km) zones was based on the DEM and on the calculation of the gravity effect of topography using vertical prisms.

After applying the necessary reductions, the standard Bouguer anomaly was calculated using a density value of 2.5 g/cm^3. The resulting Bouguer anomaly map is presented in Fig. 5a. The Bouguer anomaly values range between 32.3 and 45.2 mGal and exhibit a

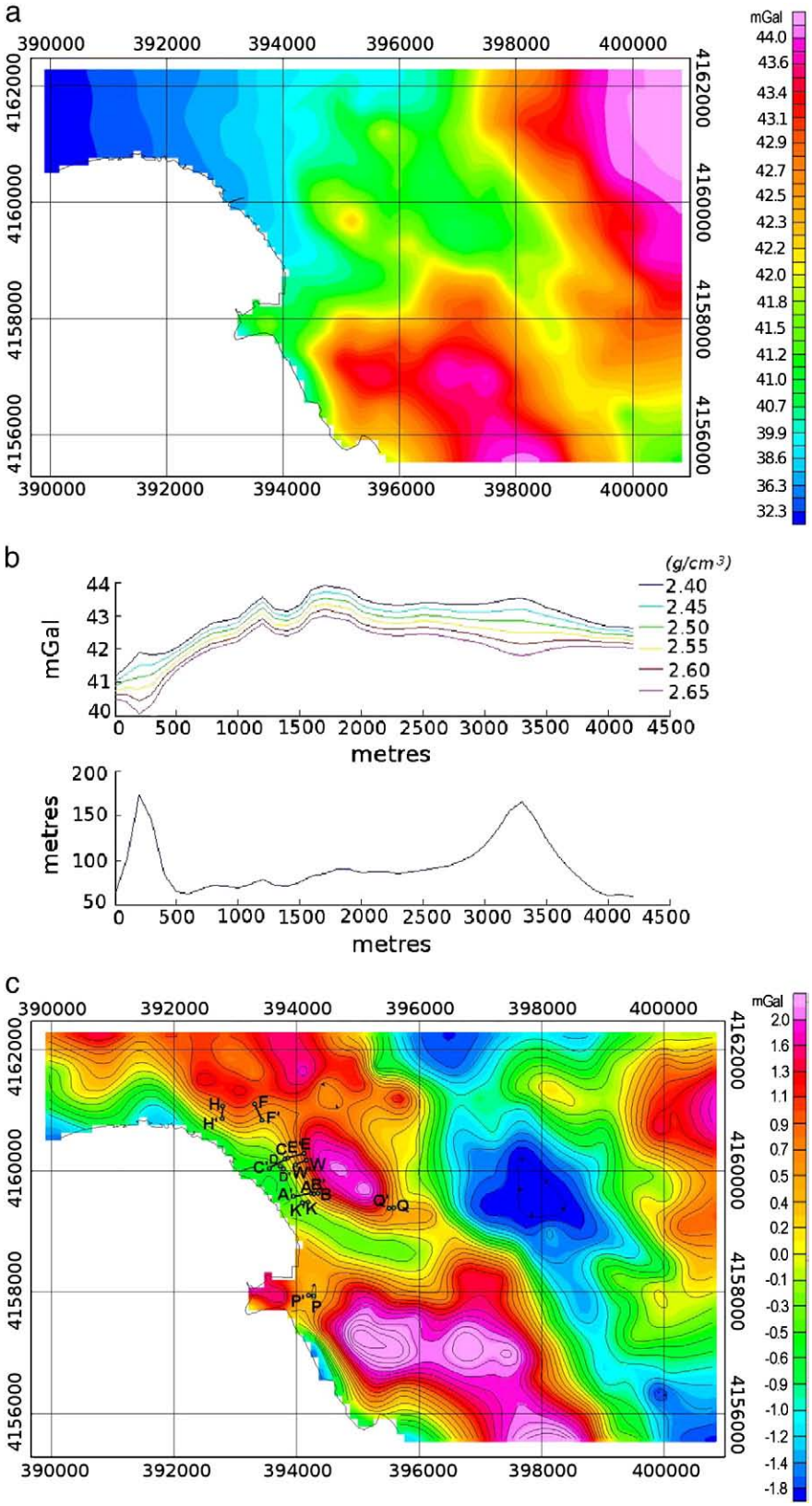

Fig. 5. (a) Bouguer gravity map of Nafplion area. The southeastern uphill trend is prominent. (b) The Nettleton method for determining the Bouguer slab density with the topography profile as shown. The most appropriate density is about 2.5 g/cm^3. (c) Residual gravity anomaly map.

Please cite this article as: Karastathis, V.K., et al., The contribution of geophysical techniques to site characterisation and liquefaction risk assessment: Case study of Nafplion City,..., J. Appl. Geophys. (2010), doi:10.1016/j.jappgeo.2010.09.003

strong southeastern uphill trend with regards to the regional field. The procedure used to choose the Bouguer slab density was based on Nettleton (1939) method (Fig. 5b). A profile was selected crossing the Southern part of the map, showing significant topography relief. The Bouguer anomaly was calculated along the profile, with density values ranging from 1.8 to 2.8 g/cm^3. The curve showing the least correlation with the topography is that produced with density value of 2.5 g/cm^3.

In order to interpret the Bouguer anomaly map in terms of local structures covered by the post-Alpine formations, it was necessary to remove the regional field component. A first order polynomial expression was fitted to the Bouguer anomaly data and the calculated values were subtracted from those observed to produce residual values. These were plotted in the form of the residual anomaly map. Fig. 5c shows the resulting residual anomaly map after the removal of the regional trend.

In the residual anomaly map (Fig. 5c), positive and negative gravity anomalies are formed. Positive anomalies appearing at the northern part of the map are related to Cretaceous carbonate formations, which are mapped as relics in the geology map. As inferred from the residual anomaly map, all these formations are interconnected beneath the post-Alpine sediments (Quaternary deposits overlying Neogene marl conglomerates, Mesozoic limestones and flysch). Further to the south, the complex of positive anomalies are not related to the Cretaceous limestones but are rather attributed to the presence of Tertiary limestones — dolomites, which form the bedrock unit of the area.

Lineaments indicated by 1 and 2 in Fig. 5c are related to probable fault structures.

Lineament 1 is located very close to Nafplion City and cross-cuts the entire area of the future expansion of the city. Further investigation using seismic methods was considered necessary in order to determine whether that lineament is associated with a fault, which presently is covered by lagoonal deposits. Relevant results are presented in the next subsection.

Lineament 2 coincides with a known inactive fault mapped in the neotectonic map produced by the Earthquake Planning and Protection Organization of Greece (Papanikolaou et al., 1996) and therefore we did not study it further.

4.1.2. Seismic survey

We conducted seismic surveys to clarify if lineament 1 (Fig. 5c) can be related to a possible fault. Each of the seismic profiles (see the map of Fig. 3) AA′, CC′, EE′, FF′ was about 300 m long while HH′ and WW′ were 180 m and 192 m long respectively. The main target of the seismic profiles was to determine the dip characteristics of the bedrock and if these could be associated to an active fault.

It must be noted that in the peripheral zone of a city, the choice of sites for the deployment of long seismic profiles, is limited by unauthorized constructions, large agricultural fields, etc. There are also limitations on the selection of the seismic source, which obviously cannot be explosives as well as on the geophone planting due to the existence of different types of obstacles (hedges, gardens, etc.).

The survey layout for the shallow seismic reflection method used was mostly the “fixed spread” instead of the usual “roll-along”. The “fixed spread” layout was not only easier in acquisition, in the physical conditions of an urban environment, but also very valuable since it permitted us to acquire data usable for joint refraction — wide angle reflection velocity modelling. A reliable velocity model is needed for depth migrating seismic data. We must bear in mind that when strong lateral velocity changes exist, as in the case of a fault presence in a seismic profile, then depth migration is preferable (see Guo and Fagin, 2002). Although the shallow reflection method has been extensively used in problems with strong lateral velocity changes, only in very few applications has poststack or prestack depth migration has been utilized (see Bradford et al., 1998, 2006; Improta and Bruno, 2007).

To determine the velocity model, the seismic 2-D traveltime inversion modelling algorithm of Zelt and Smith (1992) was primarily used. The algorithm utilizes any traveltime arrival of any seismic phase (reflection, refraction, mode-converted, etc.). Complementarily, a code of first arrival tomography (Hayashi and Takahashi, 2001) was also used for the detailed examination of the shallower sediments.

The algorithm of Zelt and Smith (1992) uses a forward traveltime modelling with ray-tracing to calculate the arrival times and an iterative inversion technique to adjust the velocity model. The velocity model parameterization is based on the consideration of velocity and boundary nodes. The number and position of velocity and boundary nodes can be adapted to the shot-receiver geometry, the ray coverage and the complexity of the near-surface geology. The velocity values in a layer result from linear relations that take into account the positions of the nodes and the boundaries. The values of velocity and boundary nodes are updated simultaneously using successive application of a ray-tracing and damped least-squares inversion algorithm.

The tomographic algorithm (Hayashi and Takahashi, 2001) is based on a ray-tracing technique with a simultaneous iterative reconstruction technique algorithm for inversion. The velocity model was constructed by many thin layers composed of quadrangle cells of uniform velocity value. The first arrival traveltimes and ray paths are calculated by the ray tracing method based on Huygens' principle. The algorithm calculates the fastest ray connecting nodes defined on the boundaries of the cells.

The seismic source utilized was an accelerated dropping weight and provided us with high quality records in all the seismic lines. A new generation 24-channel seismograph (24 bit A/D) was used for the data recording. The processing of the seismic reflection profiles was performed using Seismic Unix (Stockwell, 1999). An example record from the seismic profile HH′ is shown in “raw” format (Fig. 6a) and after band-pass filtering (50–400 Hz) (Fig. 6b). The band-pass filtering eliminated ground-roll leaving the reflection event to be dominant in the record. The remaining air-wave was easily suppressed by stacking.

Joined lines EE′ and CC′ run perpendicular to the strike of the gravity lineament 1 (Fig. 5b). The geophone interval was 12 m. The first arrivals of the refracted waves in both profiles after tomographic processing were unable to describe the bedrock. However the arrivals of reflected waves were processed by the code of Zelt and Smith (1992), and produced velocity models with excellent fitting between calculated and observed arrival times. The resultant velocity models (Fig. 7a) indicate a fairly smooth layering to the bedrock. The bedrock is detected at 90 m depth at the beginning of line EE′ and reaches 200 m at the end of line CC′. These results are in agreement with the lithology observed during the construction of an old water-well (E10 in Fig. 3) at the starting edge of EE′, which intersected the limestone bedrock at a depth of 93 m (Fig. 8).

Fig. 7b shows the joint time migrated profile after simple depth conversion.

Two layers can be distinguished above the bedrock at line CC′. The second layer, consisting probably of consolidated clay, pinches out within the line EE′, but this cannot be resolved due to the limitation of the vertical resolution. The vertical resolution according to Rayleigh criterion is about 12 m since the dominant frequency of the signal is about 50 Hz. Thus, the two pinching-out reflectors cannot be resolved when their distance is close to this resolution limit. In the EE′ profile, where the fixed spread layout has been used, all the seismic records contain traces with reflections from the poor resolution area. However, the area of the pinching-out was detailed investigated by the high resolution seismic reflection profile WW′ (see the map of Fig. 3), conducted in parallel direction to EE′ and at a very short distance.

Fig. 7c shows the resulting profile after Kirchhoff poststack depth migration with the use of the velocity model of Fig. 7a. The slope of the bedrock surface is steeper at the depth migrated profile. We alternatively applied also the Kirchhoff prestack depth migration

Please cite this article as: Karastathis, V.K., et al., The contribution of geophysical techniques to site characterisation and liquefaction risk assessment: Case study of Nafplion City,..., J. Appl. Geophys. (2010), doi:10.1016/j.jappgeo.2010.09.003

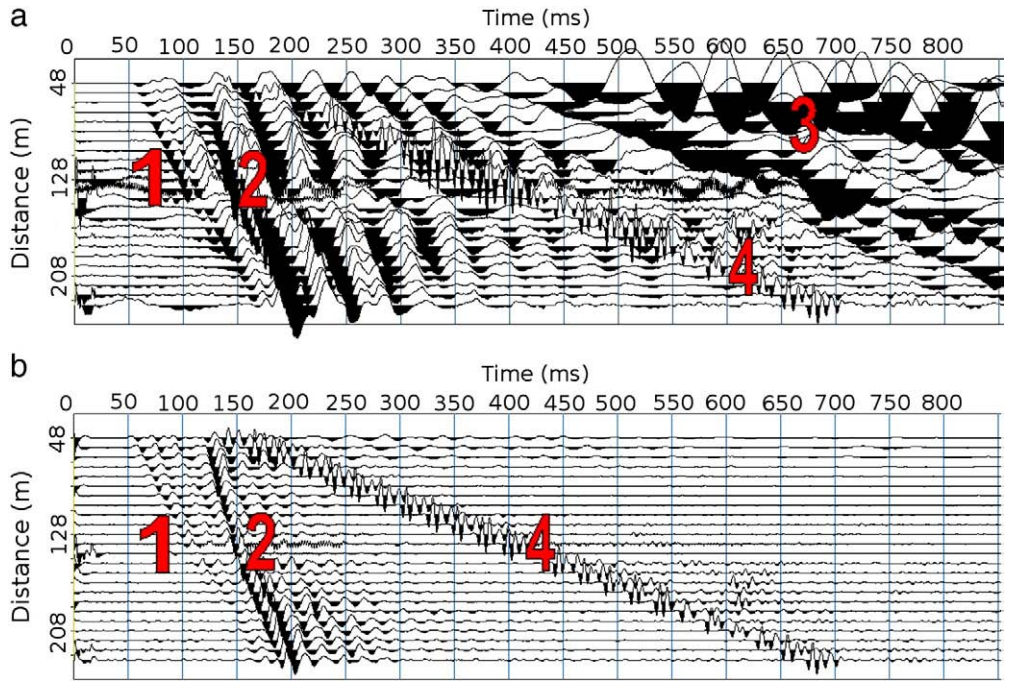

Fig. 6. Example of seismic record from the seismic profile HH′ (a) in "raw" format and (b) after band pass filtering. The reflection event is prominent at about 120 ms (indicated with the number 2). Ground-roll (indicated with 3) has been removed after filtering. However, the "airwave" noise (indicated with 4) remained since its frequency content was very high. First arrivals (refractions) (indicated with 1) also remained since their frequency content is not much lower than reflections' one.

instead of the poststack one. The dip of the bedrock surface was almost identical; however the quality of the final section was much poorer.

The results of the depth migration (Fig. 7c) of the EE′ and CC′ lines suggest that the lineament detected by the gravity survey is caused by two smooth subsidence features of the bedrock at the starting parts of CC′ (from the beginning of the profile to a distance of 100 m) and EE′ (from the start to a distance of 100 m). Both dip values are approximately 25° and are considered too small to correspond to active seismic fault. It is noted that apparent dips are measured (probably at a direction different than the one of the bedrock gradient). Assuming that the strike of the gravity contour lines follow that of the sloping bedrock, the EE′ profile is at an angle of 8°–17° with this. The line CC′ is almost orthogonal to the gravity contour lines. Therefore, after simple geometric calculations we can estimate the

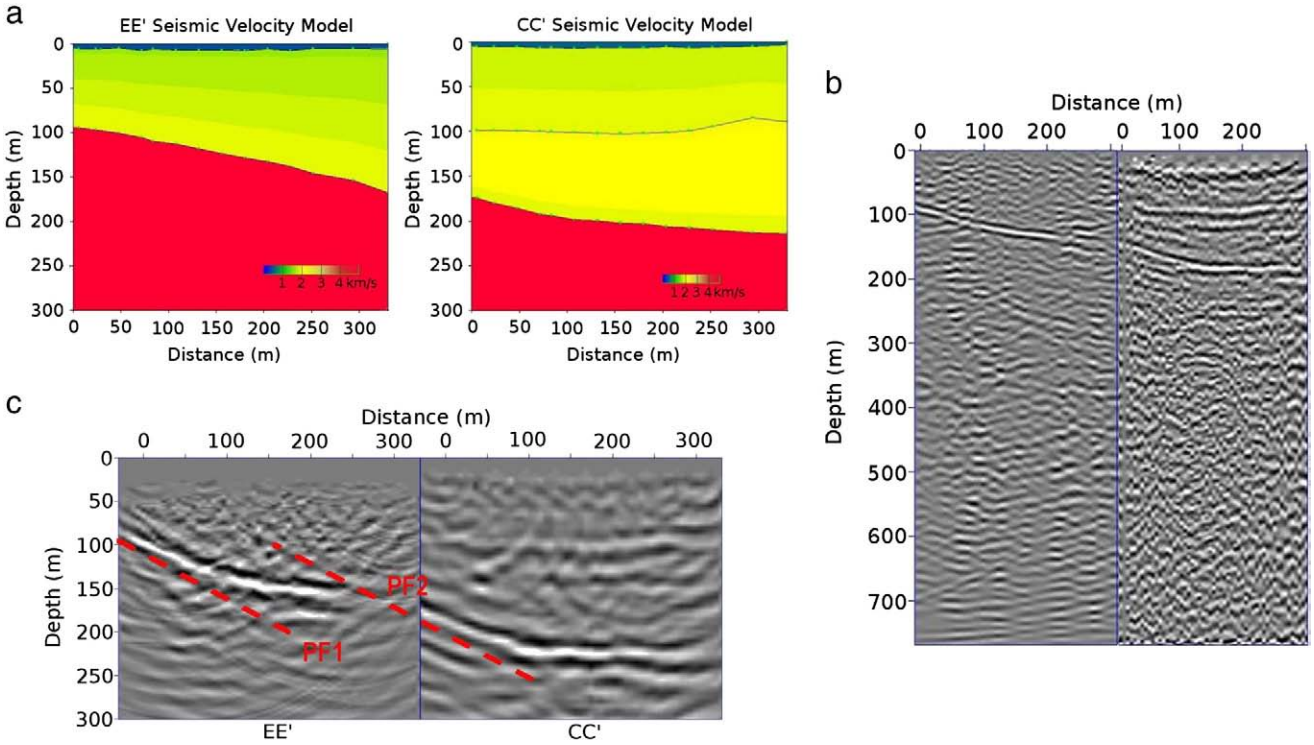

Fig. 7. (a) Velocity models of EE′ and CC′ seismic profiles. (b) Time migrated and depth converted joined seismic section of the profiles EE′ and CC′. (c) Kirchhoff depth migrated sections profiles EE′ and CC′. The suspected possible faults are indicated with PF1 and PF2.

Please cite this article as: Karastathis, V.K., et al., The contribution of geophysical techniques to site characterisation and liquefaction risk assessment: Case study of Nafplion City,..., J. Appl. Geophys. (2010), doi:10.1016/j.jappgeo.2010.09.003

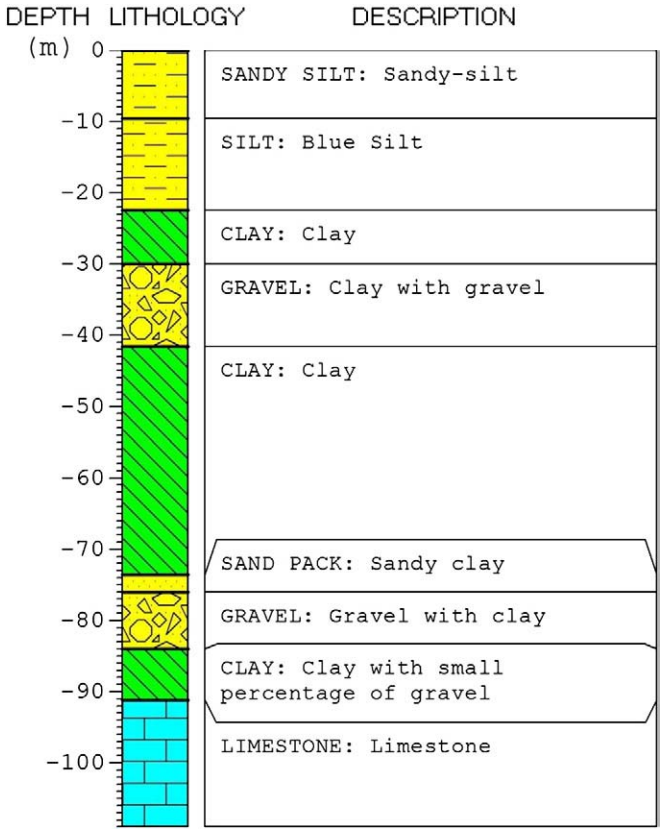

Fig. 8. The old water-well E10 located at the northern end of the profile EE′.

real value of the dip up to 26°. The apparent dip α and the real one β are simply related with the following relation

$$\tan\alpha = \tan\beta \cdot \cos\theta \quad (1)$$

where α is the apparent dip, β the real dip and θ the angle between the profile direction and the vertical to the fault direction.

Even if this slopping surface is associated with a normal fault (PF2 in Fig. 7c), this can hardly be considered as an active one. In general, low-angle normal faults (dip<30°) are considered to be incapable of causing strong earthquakes (Anderson, 1942; Jackson, 1987). However, recent geophysical and seismological studies (Wernicke, 1995; Abbott et al., 2001) do not exclude the seismic potential of such active faults. In our case, the recorded seismicity of the wider region of the Argolikos Gulf does not support any considerable potential associated with low-angle normal faults and, thus, the question of an active fault zone can be farther weaken.

However, to fully ascertain if this structure is related to an active fault, we examined if the near surface layers have been affected by the possible fault PF2 (Fig. 7c). This examination was performed by the high-resolution seismic reflection profile WW′. The profile was conducted in parallel direction to EE′, 130 m far from this, at the borders of a square with workers residences. The position of WW′ was also suitable to describe the pinching out of the deeper sedimentary layers on the dipping surface of the limestone bedrock. The geophone spacing was 6 m and the pattern followed was a combination of fixed spread with roll-along (Fig. 9a). According to Fig. 7c if the morphological characteristic PF2 was related to an active fault this would have affected the overlying sediments, something that could be clearly shown in WW′. However, the time section of Fig. 9b shows that the shallow reflectors are unaffected from a seismic activity. More specifically the reflector at about 60 ms (about 40 m depth) that can be attributed to an interface between sands and clays, is almost horizontal. The shallow sediments would have been affected either by the activation of PF1 or PF2, since the faults would be actually in the same faulted zone. Consequently, the case that of an active fault in the area cannot be farther supported.

In the processing of WW′ profile (Fig. 9b) beyond the basic steps, band-pass filtering was applied on the field records (50–500 Hz) and also trace editing, FK filtering and residual statics. The implementation of the poststack deconvolution (Fig. 9c) improved the section by the wavelet shortening (whitening of the bandwidth). The spiking deconvolution was initially tested but since it was degrading the section, a minimum lag of about 14 ms was finally used. The depth converted section is shown in Fig. 9d. The dip of the bedrock interface is about 25–26° in this section in accordance with the other sections.

In seismic profile AA′ (Fig. 10), and specifically at the beginning of the profile, a smaller dip of the bedrock interface was observed (about 20°) but taking into account the fact that the profile forms an angle of 26° with the contour lines, the actual dip can be calculated higher (23°). Fig. 10 presents also a comparison between the poststack depth migrated section and the respective prestack depth migrated one. The dip of the bedrock is the same in the two sections; however the first one is superior according to the quality of the final section.

In profile FF′ the bedrock has been detected at a depth of about 100 m, dipping gently to SE down to a depth of about 150 m. In this profile the pinch out of the consolidated clay layer was also confirmed. This structure was better described by the velocity modelling (Fig. 11) since this made possible the usage of the reflection arrivals from the top of this clayey layer.

Profile HH′ was acquired with the roll-along technique, with shot and geophone interval of 8 m, in an open flat land in favourable conditions. The same picture as in the previous profiles was derived from the final section (see Fig. 12). Fig. 12 presents some of the results of the seismic processing of line HH′. The unmigrated stack (Fig. 12a) shows a clear horizon for the bedrock interface. We also tried poststack (Fig. 12b) and prestack spiking (ungapped) deconvolution (Fig. 12c) with almost similar results. The maximum lag was chosen to be about 22 ms after examination of the autocorrelation spectra of the input data. On the deconvolved section (poststack) we applied depth conversion based on the velocity file of the velocity analysis. The velocity analysis was based on the semblance spectra examination of the CDP gathers. The resulted section (Fig. 12d) can be directly compared with the time migrated and depth converted section (Fig. 12e). The time migration was adequate since the velocity model has no strong lateral variations. The slopes in the migrated section were much steeper. Generally the bedrock dips at 26° but at a point in the middle the dip reaches 34°. Taking into account the angle that the HH′ forms with the contour lines the dip should not exceed 37°.

In conclusion, the linear features observed in the Bouguer gravity map cannot be related to active seismic faults. In the worst case, it can only be related to small and low-angle dipping inactive faults.

4.1.3. Correlation of the seismic sections with gravity profiles

In order to fully correlate the results of the gravity survey with the ones of the seismic techniques at the place of lineament 1, we conducted a more detailed microgravity survey along the seismic lines EE′ and CC′. The spacing of the successive gravity stations was 10 m.

The data were processed by the use of the modelling algorithm Grablox (Pirttijärvi, 2009). Grablox computes the gravity anomaly of a 3-D block model. The model is divided into smaller brick-like elements of varying size and individual density value. The program can be implemented for both forward and inversion modeling in 3-D and 2-D mode. The inversion procedure can optimize the density values or the height of the elements in order to optimize the fitting between measured and calculated gravity data.

The block model assumed a total height (dZ value) of 300 m and this was divided into 10 minor blocks of height (dz) 30 m. Three layers

Please cite this article as: Karastathis, V.K., et al., The contribution of geophysical techniques to site characterisation and liquefaction risk assessment: Case study of Nafplion City,..., J. Appl. Geophys. (2010), doi:10.1016/j.jappgeo.2010.09.003

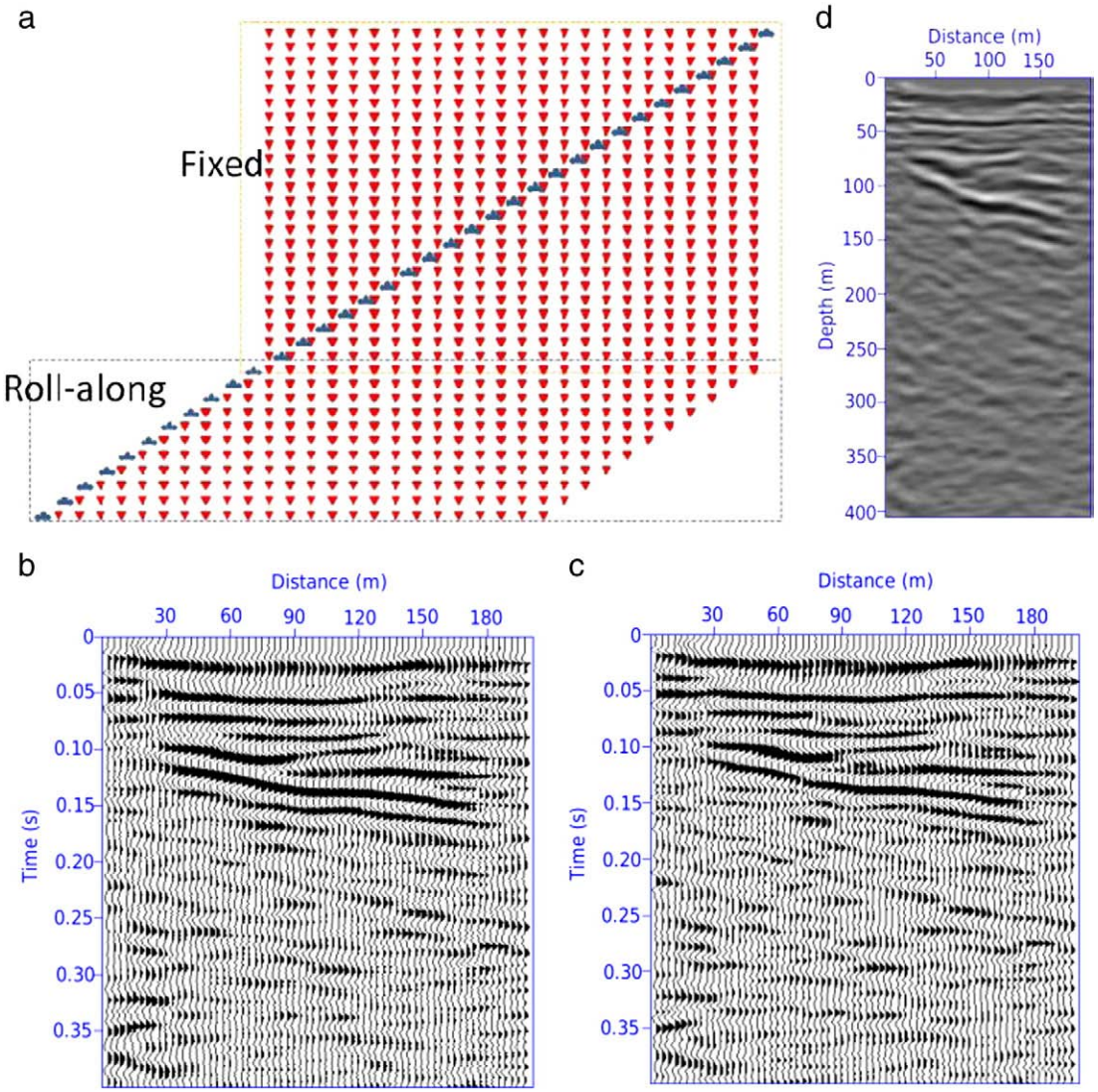

Fig. 9. (a) The data acquisition of WW′ was based on both fixed and roll-along patterns. (b) Stack section of WW′. The CDP interval is 3 m. (c) The same section after poststack deconvolution. (d) The WW′depth section.

were assumed with density values of 2.0 g/cm^3 for the saturated near surface sediments, 2.1 g/cm^3 for the deeper consolidated clay sediments and 2.5 g/cm^3 for the bedrock. The inversion routine that was used in our case optimized the height of the individual blocks using the Occam's principle, minimizing the roughness of the model. Fig. 13 shows the resulted model and the fit between the computed gravity values and the measurements.

The resulted model is in full accordance with seismic sections EE′, CC′ and WW′ and can absolutely justify the gravity measurements. Similar structure can be expected along the entire length of lineament 1.

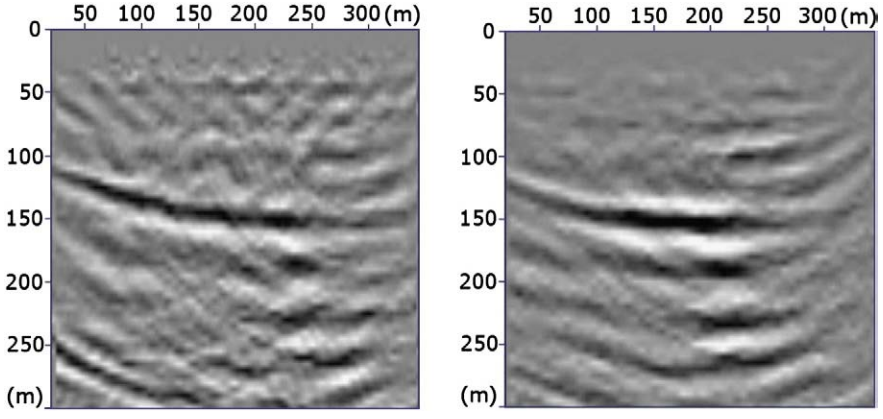

Fig. 10. Poststack (left) and Prestack (right) depth migrated sections of AA′.

Please cite this article as: Karastathis, V.K., et al., The contribution of geophysical techniques to site characterisation and liquefaction risk assessment: Case study of Nafplion City,..., J. Appl. Geophys. (2010), doi:10.1016/j.jappgeo.2010.09.003

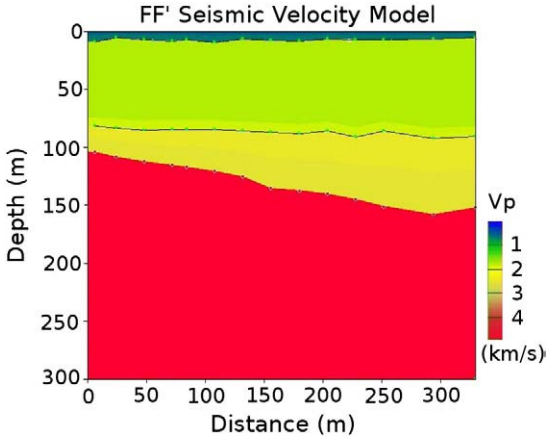

Fig. 11. The velocity model of the seismic profile FF′.

4.2. Geophysical investigations for the characterisation of the foundation ground

In order to provide a geotechnical description of the foundation ground, crosshole seismic tests were conducted at two sites within the study area, along with Standard Penetration Testing (SPT) and laboratory tests on borehole core samples.

In addition, seismic surveys were jointly carried out between the boreholes in a way to fill in the study area with the adequate information. In Fig. 3 we have mapped the lines of all conducted seismic surveys. At BB′, DD′, KK′, PP′, QQ′ we applied the methods of seismic refraction of P and S-waves and Multichannel Analysis of Surface Waves (MASW) (Park et al., 1999). In addition, at the sites AA′, CC′, EE′, FF′, HH′ and WW′, where the long seismic reflection and refraction data were acquired, we also applied MASW. At sites where information for deeper layers was required, we also acquired data for multichannel analysis of microtremors. The sites of the boreholes G1, G2 and 3042 were such sites.

The seismic crosshole tests were conducted according to the American Society for Testing and Materials standards (ASTM D4428/D4428M-07) at the sites G1 and G2 (see Fig. 3). At each site a pair of boreholes was drilled at 5 m distance, and down to a depth of 40 m. A sparker was used as seismic source and a 3-component geophone as a receiver. The results of both the crosshole tests and their borehole logs are presented in Fig. 14. The shear wave seismic velocity values in the loose sandy-silt and clayey silt intercalated formations did not exceed 0.4 km/s, but moreover there are parts with values even lower than 0.2 km/s. The P-wave velocity was high (higher than 1.5 km/s) due to the saturation from the seawater intrusion in the area.

At the site of borehole G2 (see Fig. 3) we conducted also Reverse Vertical Seismic Profile (RVSP) modelling with the seismic source in the borehole and the receivers at the surface. The results of the applied tomographic algorithm (Hayashi and Takahashi, 2001) were

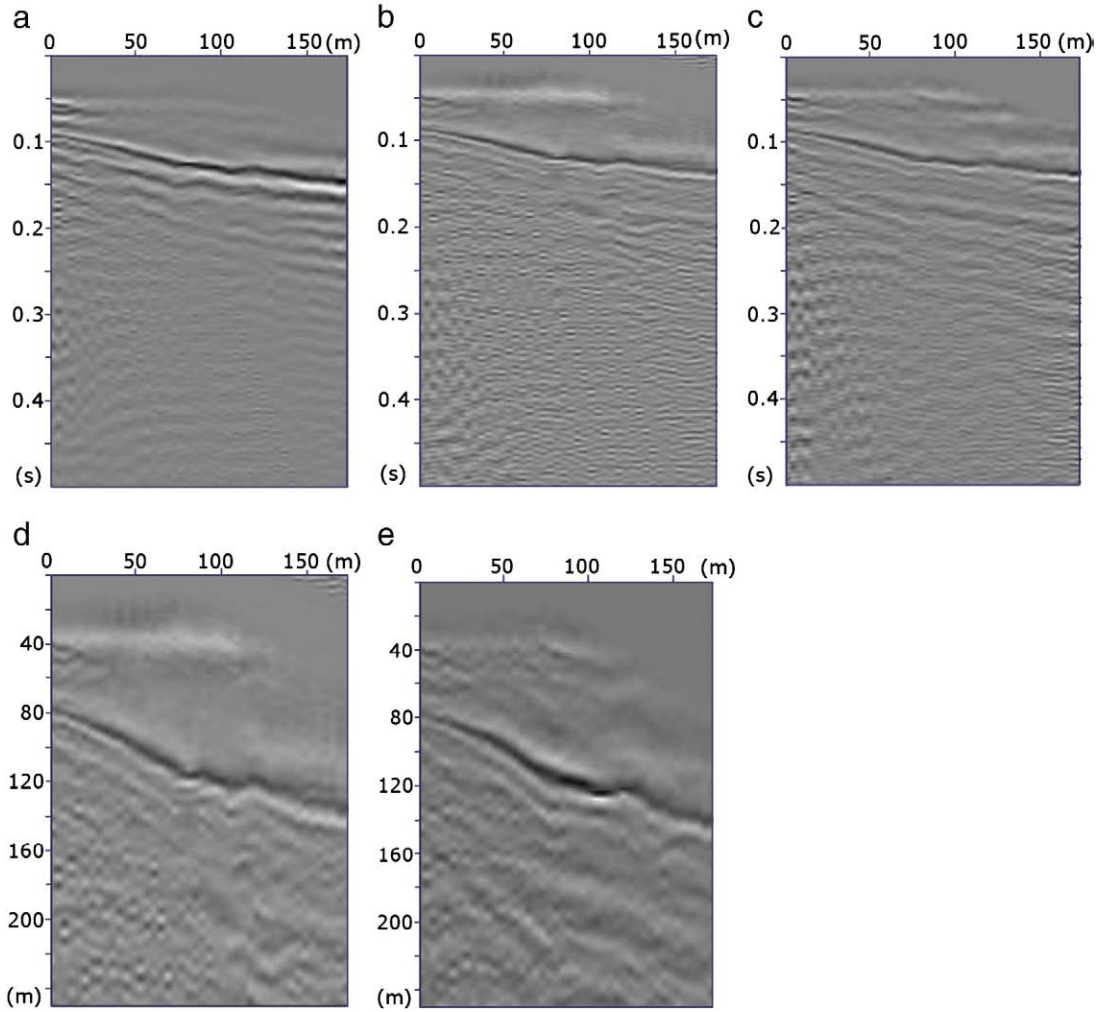

Fig. 12. (a) Unmigrated stack section of the profile HH′. (b) A section after poststack deconvolution. (c) A section resulted after processing with prestack deconvolution. (d) The deconvolved section (poststack) after depth conversion. (e) Time migrated and depth converted section.

Please cite this article as: Karastathis, V.K., et al., The contribution of geophysical techniques to site characterisation and liquefaction risk assessment: Case study of Nafplion City,..., J. Appl. Geophys. (2010), doi:10.1016/j.jappgeo.2010.09.003

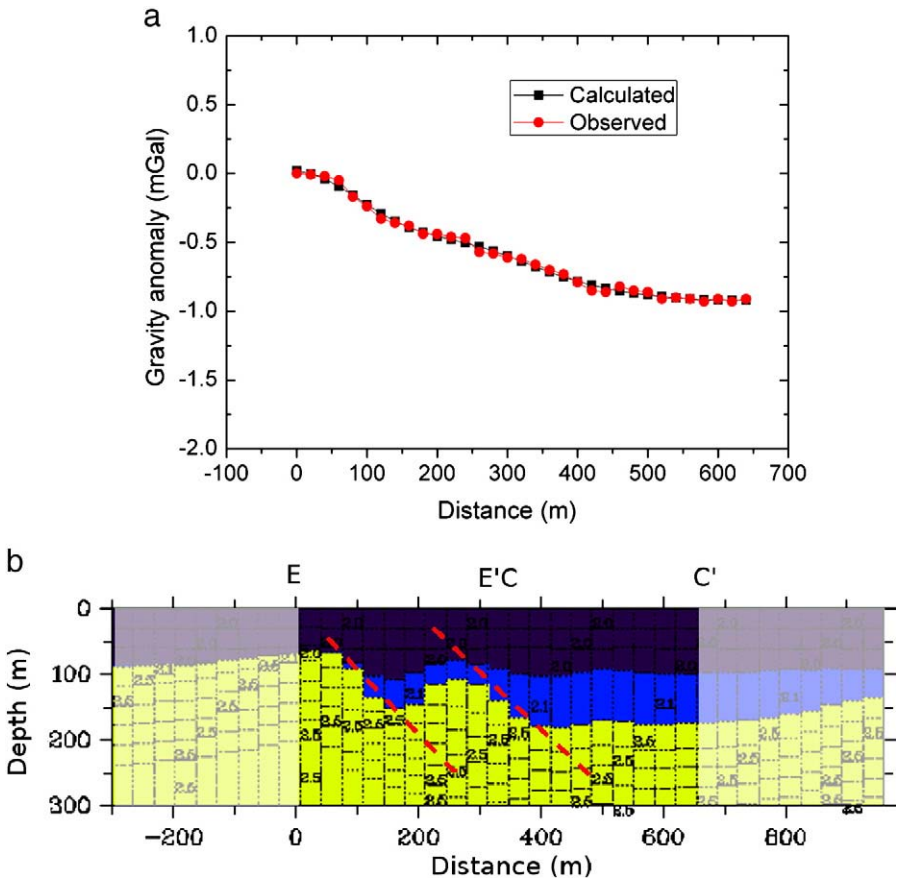

Fig. 13. (a) The fit between the calculated gravity data and the measurements was very good in the gravity profile EE′CC′. (b) The resulted model.

excellent and it was found that the drilling of the second hole could be spared. Fig. 15 shows the result of the RVSP modelling and a comparison diagram with the crosshole test. A small deviation at the depth of 31 m can be attributed to the false interpretation of crosshole testing that measured the arrival of a refracted wave instead of a direct one. RVSP has also the advantage of covering a much larger part of the investigation area.

The crosshole testing and RVSP were also used to calibrate and validate the results of the other seismic surveys conducted for the geotechnical evaluation of the foundation ground.

The application of MASW yielded satisfactory results and detected the shallow low S-wave velocity zones. At a close distance to G2 borehole we applied MASW and the results were in full accordance with the crosshole test.

The 1-D distribution of the shear wave velocity, from the microtremor array measurements using the spatial autocorrelation method (Okada, 2006; Roberts and Asten, 2004), did not provide the level of the drilling precision (Roberts and Asten, 2005), although is in very good agreement with the results of the crosshole testing at shallow depths and moreover provides information for deeper layers (Fig. 16).

As shown in Fig. 17a the S-wave velocity presents low values in the top 10 m within the entire investigated area (at least 1 km^2). This is also found from S-wave seismic refraction profiles. Fig. 17b shows an example of the typical fundamental dispersion curve from the MASW surveys.

From information derived from the local boreholes (G2 shown in Fig. 14 and E10 shown in Fig. 8) the layer corresponding to the low S-wave velocity values is a sandy-silt to silty-sand, soft formation without plasticity. From the laboratory analysis, sand concentrations of 29% and 66% at 4.90–5.55 m and 7.90–8.55 m depth respectively were found. The concentrations of clay were considerably low, of the order of 1% and 5% respectively. This evidence supports the high liquefaction susceptibility of the area.

The sandy-silt or silty sand layer is described also in the S-wave seismic refraction profiles with velocity values up to 0.2 km/s. The corresponding P-wave profiles describe this low-velocity formation only down to the saturation depth (3–8 m), depending on the distance from the sea.

5. Assessment of the liquefaction risk

In this section we use the data and new information derived by the application of the various geophysical methods in the area of Nafplion to assess the liquefaction potential at eight selected sites. All eight sites AA′, BB′, CC′, DD′, EE′, WW′, G1, and G2, are located within the area of urban expansion of the city of Nafplion (locations are shown in Fig. 3).

In addition to the information provided by the geophysical measurements, the assessment of the liquefaction risk requires a value of the expected Peak Ground Acceleration (PGA) at each one of the sites. To obtain such values for our eight study sites, we applied a stochastic strong ground motion simulation technique for several earthquake scenarios.

The synthetic PGA values were subsequently incorporated in the assessment of the liquefaction potential and more specifically in the computation of the Factor of Safety (FS) against liquefaction and the potential for liquefaction in terms of probability (P_L).

As a final step we computed liquefaction time histories for those sites that were found to be liquefiable, using a nonlinear, effective stress site response analysis (Matasovic, 2006), capable of modelling pore water pressure generation and dissipation.

The three aforementioned steps of our analysis are further described in the following sub-sections.

Please cite this article as: Karastathis, V.K., et al., The contribution of geophysical techniques to site characterisation and liquefaction risk assessment: Case study of Nafplion City,..., J. Appl. Geophys. (2010), doi:10.1016/j.jappgeo.2010.09.003

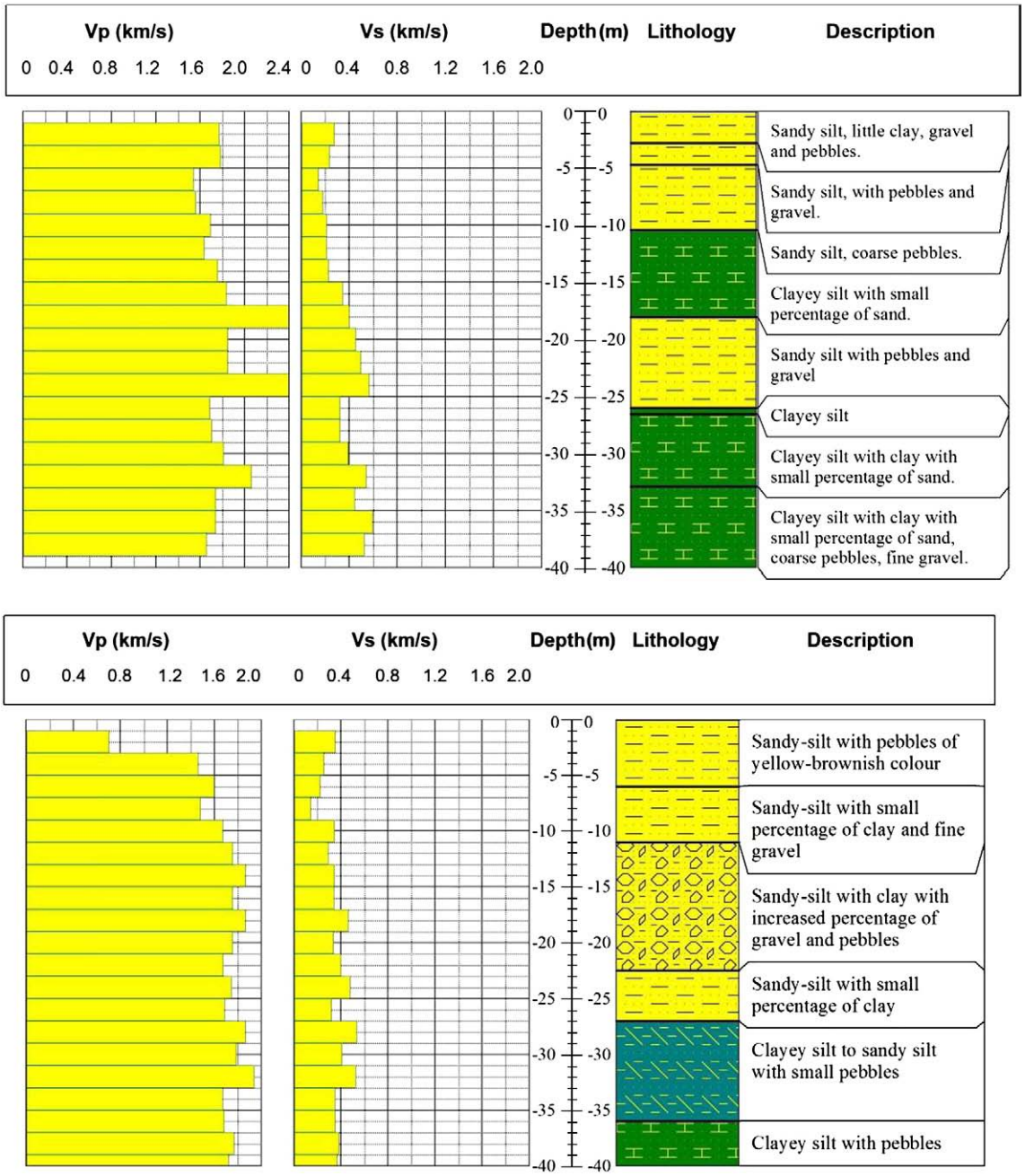

Fig. 14. The results of the crosshole testing at the sites of the boreholes G1 (above) and G2 (below).

5.1. Determination of earthquake scenarios and simulation of strong ground motion

After the establishment of profiles the next step was to estimate input motion from scenario earthquakes that could affect the study area.

Earthquake scenarios were selected on the basis of the available historical and instrumental seismicity data. From the seismic history of the area (Papazachos and Papazachou, 2003) we found three strong earthquakes events that reportedly affected the built environment of the city of Nafplion. These earthquakes have been related to the known faults (Fig. 4) and were selected for simulation:

1. Scenario earthquake of M6.3 on the Epidaurus fault
2. Scenario earthquake of M6.4 on Iria fault
3. Scenario earthquake of M6.7 on Xylokastro fault

To simulate the strong ground acceleration at the sites of interest we applied the stochastic method for finite sources as has been proposed by Beresnev and Atkinson (1997, 1998). The specific method was chosen due to its simplicity in application since available information on the earthquake sources and the regional and local seismic wave attenuation characteristics do not permit a more deterministic approach. Furthermore, the applicability of the method has been shown in past studies to be quite successful throughout a wide range of frequencies and in various seismotectonic environments (e.g. Hough et al., 2002; Boore, 2003 and references therein; Roumelioti and Beresnev, 2003; Castro and Ruiz-Cruz, 2005).

The applied method involves discretisation of the fault plane into a certain number of subfaults, each of which is assigned an ω^{-2} spectrum. Each subfault is triggered when the rupture front reaches it. Contributions from all subfaults are empirically attenuated to the observation site and appropriately summed to produce the synthetic

Please cite this article as: Karastathis, V.K., et al., The contribution of geophysical techniques to site characterisation and liquefaction risk assessment: Case study of Nafplion City,..., J. Appl. Geophys. (2010), doi:10.1016/j.jappgeo.2010.09.003

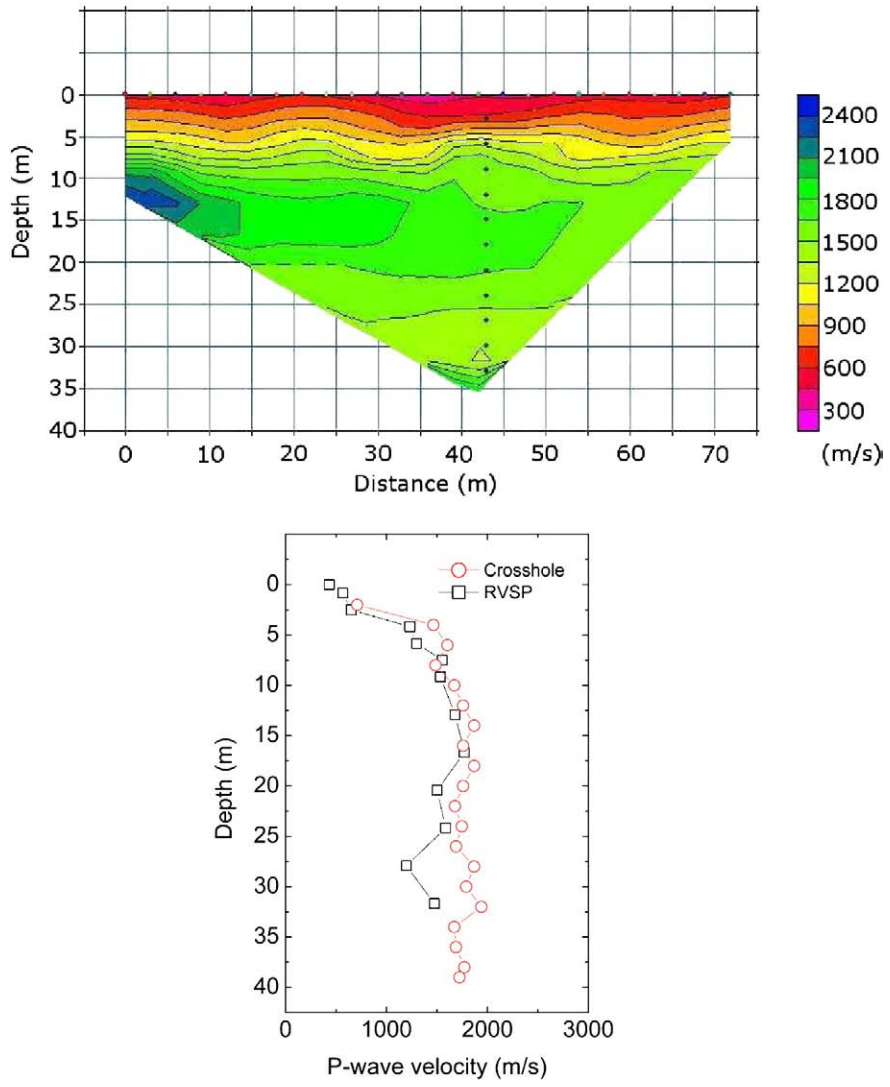

Fig. 15. Above: The velocity model of RVSP at the site KK′. Below: Comparison of RVSP with crosshole testing.

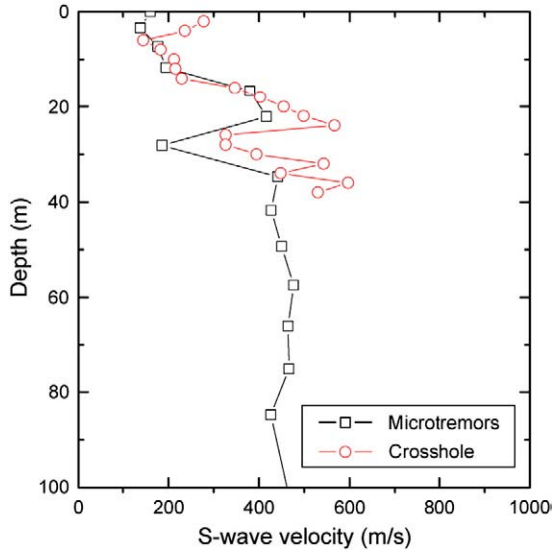

Fig. 16. The results of multichannel analysis of passive recording (microtremors) at the site G1 fit quite well with the respective results of the crosshole testing at the shallow depths (if we take into account the difference in the resolution of the methods), and complement the Vs variation for the deeper structure.

accelerogram. For a detailed description of the applied method and the parameters involved in its application (FINSIM code) readers are referred to the original work of Beresnev and Atkinson (1997, 1998). Herein, for reasons of economy, we only present Table 1 with the values of all simulation parameters for each one of the three examined earthquake scenarios. In Fig. 4 we also present the surface projections of the three fault models as they were adopted in the applied simulation method.

The product of the stochastic simulations was a set of synthetic acceleration time histories (S-wave part only) at the eight sites of interest. The PGA values of these synthetic waveforms are included in Table 2.

5.2. Calculation of the Factor of Safety (FS) against liquefaction, and estimation of the potential for liquefaction in terms of probability (P_L)

The results of the stochastic strong ground motion simulation were subsequently exploited in the assessment of the liquefaction risk. To calculate *FS* at the selected sites, we used the shear-wave velocity Vs profiles of the top 30 m of the soil column as were determined from the surface-wave method and the crosshole tests previously described. The depth of the water table was defined by the seismic refraction technique (Fig. 18) and the values of the horizontal PGA resulted from the stochastic strong ground motion simulation.

Please cite this article as: Karastathis, V.K., et al., The contribution of geophysical techniques to site characterisation and liquefaction risk assessment: Case study of Nafplion City,..., J. Appl. Geophys. (2010), doi:10.1016/j.jappgeo.2010.09.003

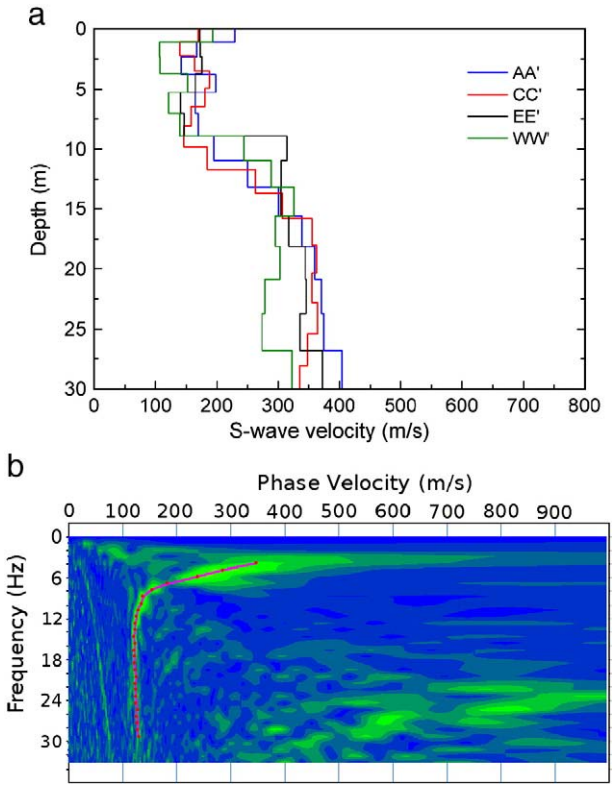

Fig. 17. (a) MASW results systematically showed low S-wave velocity values at the top 10 m of the soil column. (b) Example of a dispersion image from the MASW records. The fundamental mode phase velocity curve is shown on the spectrum with a red line. (For interpretation of the references to colour in this figure legend, the reader is referred to the web version of this article.)

The applied method to determine *FS* is particularly useful in soils that are difficult to be sampled, such as gravelly soils, where penetration tests may be unreliable, and at sites where drilling may not be permitted, such as capped landfills. Another advantage of the Vs approach is the direct estimation of several other dynamic parameters related to the seismic velocity.

FS is usually expressed as the ratio of the cyclic resistance (*CRR*, soil "strength") based on in-situ test data (i.e. SPT, BPT, CPT) to the average cyclic stress (*CSR*, earthquake "load") induced in the soil by an earthquake: $FS = CRR/CSR$. The earthquake demand (*CSR*) was calculated by the Seed's method (Seed and Idriss, 1971), through the equation:

$$CSR = 0.65\frac{\sigma_0}{\sigma_0'}a_{\max}r_d \quad (2)$$

where 0.65 is a weighing factor, introduced by Seed, to calculate the number of uniform stress cycles required to produce the same pore water pressure increase as an irregular earthquake ground motion; σ_0 is the total vertical overburden stress; σ_0' is the effective vertical overburden stress based on water table during earthquake; $a_{\max}$ is the horizontal PGA (in g units); r_d is the stress reduction coefficient, which is varying with depth.

The value of r_d at the depth of z can be calculated using the following equation (Youd and Noble, 1997):

$$r_d = 1.0 - 0.00765z \text{ for } z \le 9.15 \text{ m};$$
$$r_d = 1.174 - 0.0267z \text{ for } 9.15 \text{ m} < z \le 23 \text{ m};$$
$$r_d = 0.744 - 0.008z \text{ for } 23 \text{ m} < z \le 30 \text{ m};$$

The equation for determining the *CRR* from Vs is empirical and based on case history studies at sites that did and did not liquefy during earthquakes (Andrus and Stokoe, 1997, 2000):

$$CRR = 0.022(K_C V_{S1}/100)^2 + 2.8(1/(V_{S1C} - K_C V_{S1}) - 1/V_{S1C})\cdot MSF \quad (3)$$

where, $MSF = (M_w/7.5)^{-2.56}$ is a magnitude scaling factor; V_{S1} is the stress-corrected V_S and defined as $V_{s_1} = V_s(Pa/\sigma_v')^{0.25}$; where V_s is the measured shear-wave velocity (m/s), *Pa* is the reference stress (100 kPa), σ_v' is initial effective overburden stress (kPa); V_{S1C} is a correction factor that depends on fines content; K_c is a correction factor for cementation and aging and M_w is the earthquake moment magnitude.

Table 1
Parameters adopted in the stochastic simulation of strong ground motion from three scenario earthquakes in the broader area of Nafplion City (see text for further information on the selected scenario events).

Parameter	Symbol	Scenario 1 (M6.3)	Scenario 2 (M6.4)	Scenario 3 (M6.7)
Fault orientation	Strike, φ	275°	266°	295°
	Dip, δ	43°	48°	30°
Fault dimensions	Length, L (km)	19	21	30
	Width, W (km)	12	13	16
Depth to upper edge of the fault	h (km)	1.0		
Hypocenter location on the fault	i_0, j_0	6, 3 Forcing rupture directivity toward the city of Nafplion		4,3 Central and lower part of the fault
Stress drop	Stress (bars)	50.0		
Number of subfaults along strike and dip	$NL \times NW$	6×4	6×4	6×3
Crustal shear wave velocity	Beta (km/s)	3.7		
Crustal density	Rho, g/cm^3	2.72		
Parameter controlling high-frequency level	sfact	1.5		
Parameter k_0	kappa	Depending on the site category of each observation point 0.035 (site class B)		
Parameter of the attenuation model $Q(f) = Q_0{}^*f^{**}eta$	Q_0	100.0		
	eta	0.8		
Geometric spreading	igeom	0 (1/R model)		
Distance-dependent duration (s)	rmin	10.0		
	rd1	70.0		
	rd2	130.0		
	durmin	0.0		
	b1	0.16		
	b2	−0.03		
	b3	0.04		
Windowing function f_m (Hz)	iwind	1 (Saragoni–Hart window)		
Slip distribution model	islip	Random		

Please cite this article as: Karastathis, V.K., et al., The contribution of geophysical techniques to site characterisation and liquefaction risk assessment: Case study of Nafplion City,..., J. Appl. Geophys. (2010), doi:10.1016/j.jappgeo.2010.09.003

Table 2
The liquefaction potential estimated for different sites of Nafplion City.

Sites	PGA (g)	Ground water level (m)	Depth interval (m)	Factor of safety against liquefaction	Probability of liquefaction (%)
Earthquake scenario with magnitude M = 6.4 on the Iria fault					
AA′	0.164	4	6–13	1.01–0.42	25–86
BB′	0.186	4	5.8	0.93	30
CC′	0.217	5	2.2–9.6	0.73–0.21	50–99
DD′	0.217	3	5–11.9	1.19–0.69	16–54
EE′	0.179	5.8	7.7–15.8	1.07–0.78	21–44
G1	0.146	2	6.0	0.22	98
G2	0.146	2	4–7	1.29–0.27	13–97
WW′	0.124	4.2	8	1.2–0.87	20–48
Earthquake source with magnitude M = 6.3 on the Epidaurus fault					
AA′	0.050	4	6–12	0.5–2.0	40
BB′	0.053	4	5.8	2.5–1.5	0
CC′	0.036	5	6–10	0.5–2.5	60
DD′	0.047	3	5–11.9	3–4	0
EE′	0.043	5.8	7.7–15.8	4–2.5	0
G1	0.055	2	6.0	1	25
G2	0.055	2	6–8	4.0–0.73	50
WW′	0.043	4.2	8–8.5	0.5–2.0	5–10
Earthquake scenario with magnitude M = 6.7 on the Xylokastro fault					
AA′	0.045	4	6–10	0.94–2.13	29
BB′	0.045	4	5.8–10.8	1.78–3.31	5
CC′	0.045	5	6–10	0.59–0.85	37–67
DD′	0.043	3	4–9	1.69–1.77	5
EE′	0.043	5.8	7.7–15.8	2.5–3	0
G1	0.046	2	6.0–8	0.8–1.69	40
G2	0.042	2	6–8	0.79–2.98	43
WW′	0.042	4.2	8–8.5	1.6–1.9	3

In the present study we set the value of K_c equal to 1, since there is currently no widely accepted method for estimating K_c and its variability across the category areas (Andrus and Stokoe, 1997, 2000). The actual fines content varies with depth and location. However, in the analysis introduced by Andrus and Stokoe (1997, 2000), Eq. (3) was derived from sands and gravels that were classified into three broad categories with regards to fines content: ≤5%, 6%–34%, and >35%. In our case studies the contents of fines of the liquefiable sandy silt ranges from 16% to 60%.

FS is the ultimate result of the first step of our analysis. If *FS* is greater or equal to 1, there is no potential of liquefaction. However, if *FS* is less than 1, liquefaction can occur. Based on the values of *FS* at the study sites, we subsequently expressed the liquefaction potential in terms of probability. One of the important advantages of such an expression is the fact that the *probability of liquefaction* is the information required for risk-based design decision making. Probability of liquefaction is obtained using the equation suggested by Juang et al. (2001):

$$P_L = \frac{1}{1 + \left(\frac{FS}{0.73}\right)^{3.4}} \quad (4)$$

Table 2 shows the obtained values of *FS* and P_L for all the investigated sites and all three earthquake scenarios. Among the tested scenarios the one on Iria fault was identified as the worst in terms of liquefaction initiation. Relative results imply that some of the investigated sites (AA′, CC′, EE′, WW′, G1, and G2) will liquefy with high probability.

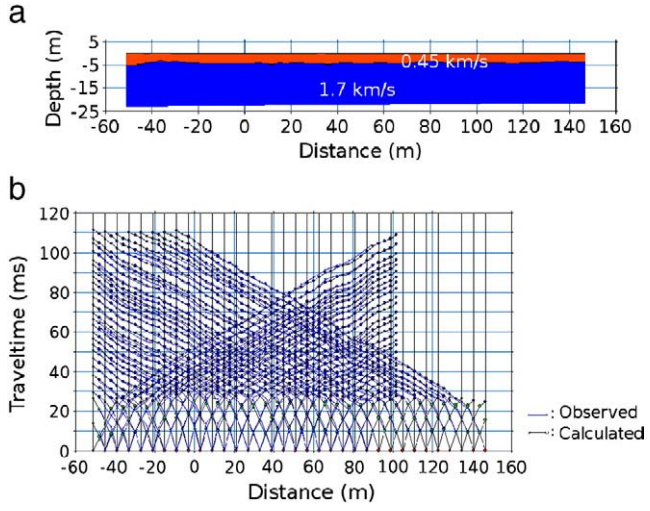

Fig. 18. An example of the water-table detection from a seismic refraction profile at the site WW′. (a) The resulted section. The velocity of the second layer is about 1.7 km/s. Since the S-wave velocity is about 0.15 km/s (see Fig. 17) the Poisson Ratio value approaches 0.5, i.e. the full saturation. (b) The fitting between the observed and calculated traveltimes was very good.

5.3. Evaluation of liquefaction time histories at the potentially liquefiable sites

To compute liquefaction time histories at the sites that present high probability for liquefaction we employed the 1-D code D-MOD2000 (Matasovic, 1993), which is capable of performing fully nonlinear, effective stress based ground response analysis (cyclic degradation of material properties with hydraulic interaction between layers, i.e., dynamic response plus pore water pressure generation plus pore water pressure dissipation and redistribution).

In comparison with the codes that account for the nonlinear behaviour of the soil using an iterative procedure, e.g. SHAKE2000 (Idriss and Sun, 1992; Ordonez, 2002), D-MOD2000 presents the following three advantages:

(i) There are no restrictions on the input acceleration level; in fact, D-MOD2000 incorporates a nonlinear constitutive model, while codes which are based on an equivalent-linear model typically extend up to 1% shear strain level. In large earthquakes and soft soils, shear strains in excess of 1.0% can be induced;
(ii) D-MOD2000 can directly calculate soil liquefaction potential given that D-MOD2000 is an effective stress program;
(iii) D-MOD2000 accommodates pore water pressure induced "soil softening" (reduction in shear modulus and strength). Among its other advantages, D-MOD2000 includes an extensive database of "ready-made" material properties.

A detailed discussion on the proper handling of measured and estimated data, which are needed to run D-MOD analysis, is given in Matasovic (1993).

The results of our analyses indicated the scenario of the activation of the Iria fault as the worst one in terms of the liquefaction potential. The Epidaurus fault also showed similar characteristics in contrast to the Xylokastro fault that did not give a high probability of liquefaction at any of the examined sites within the study area.

In cases where high liquefaction potential was predicted, synthetic ground acceleration waveforms at the surface are characterized by low PGA values but are rather enriched in longer periods. This is due to the liquefaction of soil at a certain depth.

An example of this analysis, corresponding to the $M = 6.4$ scenario earthquake on the Iria fault, is given in Fig. 19. More specifically in this Figure we show (a) the synthetic acceleration time history at the surface (b) the synthetic acceleration time history at the potentially liquefiable layer, (c) the time history and (d) the depth distribution of the pore water pressure ratio at test site AA′. In the case of this earthquake scenario, the predicted liquefaction effect (Fig. 19c, d) acts against the effect of soil amplification. Thus, ground acceleration at

Please cite this article as: Karastathis, V.K., et al., The contribution of geophysical techniques to site characterisation and liquefaction risk assessment: Case study of Nafplion City,..., J. Appl. Geophys. (2010), doi:10.1016/j.jappgeo.2010.09.003

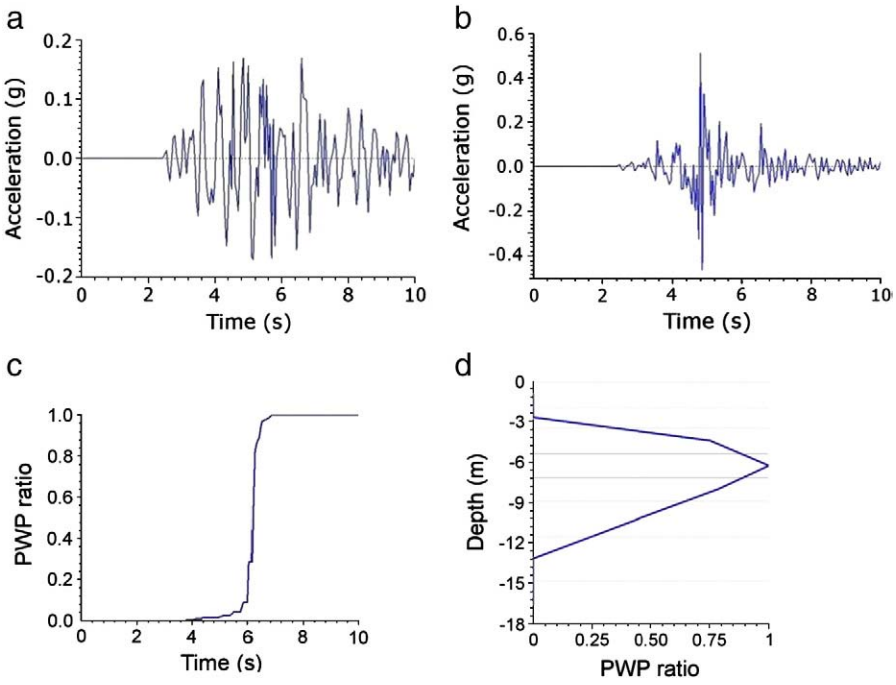

Fig. 19. Results of the liquefaction analysis for the AA′ test site of Nafplion: (a) surface acceleration time history; (b) the acceleration time history at the potentially liquefiable layer; (c) the time history and (d) the depth distribution of pore water pressure ratio.

the surface (Fig. 19a) shows lower amplitudes and longer periods compared to the respective time history at the base of the liquefied layer (Fig. 19b). For this specific earthquake scenario, the occurrence of liquefaction, in terms of probability, was high, reaching 86% at depths between 6 and 10 m (see Table 2).

6. Discussion

Geophysical investigations can have a key role in microzonation studies, especially in areas where the town planning is expanding. These investigations are usually based on shallow seismic methods, such as MASW or microtremor analysis, and aim mostly at the characterisation of the foundation ground (e.g. Anbazhagan et al., 2009; Apostolidis et al., 2004). However, the contribution of the geophysical surveys could also be extended to the systematic investigation of hidden ("blind") faults and to liquefaction risk assessment. The Greek Earthquake Resistant Design Code (2000) of the Earthquake Planning and Protection Organisation classifies the areas containing active faults, and also the ones with high liquefaction potential, as X category, i.e. the category where regular building is hindered. Since in regions of high seismicity, such as Greece, both these factors are very common, the areas that should undergo such an investigation are too wide to be covered solely by standard drilling surveys. Our opinion is that the present case study in the expansion area of the town Nafplion is a good example of how geophysical techniques can be combined with the standard methodologies to cover wide areas in a fast, inexpensive, and efficient way.

The preliminary mapping of candidate fault structures by the use of potential geophysical methods and their further investigation by seismic techniques is certainly something usual in oil and mining geophysics. However, in microzonation studies this is not a common practice. Only a few cities in Greece have gravity map coverage indicating "suspicious" structures, which could assist the work of urban planning. Nevertheless, gravity mapping on its own is not enough and needs to be complemented by seismic profiles in order to be useful for engineers. The complementary role of these two methodologies in a seismic hazard study is described also by Bexfield et al. (2006).

Herein we presented an example of how gravity surveys can offer a means of quick identification of the areas that can host probable faults (lineaments). However, even in cases of identified faults, it is difficult, using these surveys, to determine precisely the nature and their geometrical characteristics, required for further studies. For example, the dip of normal faults can be important since it can be related to their seismic activity. Another decisive parameter, probably the most important in verifying the recent activity of the faults, is the degree to which surface sediments have been affected. The input of the seismic methods is necessary to determine the detailed characteristics of the candidate faults and clarify the ambiguities left by other methods.

The gravity survey in the Nafplion case history revealed the presence of two linear anomalies which could be assigned to abrupt bedrock slopes. One of them coincides with a mapped inactive fault although the second one could not be related to any known fault structure and thus was further studied by seismic methods. Seismic methods confirmed the dipping surface of the bedrock but excluded the possibility of it being related to an active normal fault, since its dip was gentle and the overlying sediments undisturbed. This dipping surface at the bedrock could be correlated with an old buried scarp of a low angle normal fault. If the anomaly was like an abrupt step, the dip of the fault would be high and then it would be difficult to detect any reflection signal from the scarp surface. In that case, if the overlying Holocenic surface sediments had also similar steps over the same place, then we could consider the case of an active fault.

In order to precisely map the dip of a possible fault, structure usually related with lateral seismic velocity variations, pinching out of layers etc., the use of depth imaging was selected. In the present case the choice of the "fixed spread" lay-out assisted the construction of reliable velocity models, by the use of inverse modelling, and hence increased the reliability of the depth imaging. The results of the method were of high quality. We must also note that in cases where the ground-roll is very strong and of high velocity, obscuring so the reflection signal and making its processing by standard CDP techniques difficult, we can alternatively process the data by ray-tracing modelling provided that we can recognize and indentify the reflection arrivals in the records. The modelling can also be useful when the records are very noisy by ambient noise and the signal is poorly recognisable. This could give solution of

Please cite this article as: Karastathis, V.K., et al., The contribution of geophysical techniques to site characterisation and liquefaction risk assessment: Case study of Nafplion City,..., J. Appl. Geophys. (2010), doi:10.1016/j.jappgeo.2010.09.003

adequate quality without the need of further processing. It is also worth noting that the use of the depth imaging in shallow reflection data is uncommon, mainly because of the complexity of the processing (it requires a velocity model).

The seismic methods were applied successfully and in a complimentary manner to the standard geotechnical techniques, aiming to determine the variation of shear wave velocity with depth. It is useful to test geophysical techniques first at the sites of geotechnical boreholes in order to validate and calibrate their results and afterwards to apply these methods at the intermediate space. Also some old wells could become important if MASW tests could be applied nearby. The integration of old information with new can be easily achieved through geophysics.

In the present article we focused on the presentation of the results of the geophysical methods and only gave a brief example of further use of these results in the assessment of liquefaction risk at selected sites. We avoided giving highly technical information on the liquefaction assessment analysis since this was judged to be out of scope of a geophysical journal. Therefore issues such as a) the details in the application of finite-fault stochastic simulation method of strong ground motion, b) the choice of the parameters for the application of the nonlinear effective stress analysis coded in D-MOD2000, b) the dependence of soil response under dynamic loading on strain, c) the comparison of the results of the liquefaction risk assessment based on Vs with ones that were obtained using borehole testing etc., have been left for a future presentation in a geotechnical journal.

7. Conclusions

The area where Nafplion City is expanding, after its examination with realistic earthquake scenarios based on known earthquake sources associated with strong and catastrophic events in the recent past, can be considered as liable for liquefaction phenomena under certain conditions of seismic loading. The problem was mainly found at the depths of 8 to 10 m, where a loose sand-silty layer is present with particularly low S-wave velocity values. The liquefaction potential was calculated, based on the results of the geotechnical investigations, laboratory tests and the results of the seismic surveys. A high liquefaction risk is anticipated mostly for strong earthquake scenarios at Iria and Epidaurus faults.

The study area was also examined for possible unexposed faults by a combined application of gravity and seismic methods but the results cannot support the presence of active faults.

The techniques utilized in Nafplion case, can also be applied with low cost in any other site with similar conditions as far as the liquefaction phenomenon is concerned.

The results support the point of view that the modern geophysical techniques are reliable enough to be included in the standard liquefaction risk studies.

Acknowledgments

This study was implemented in the frame of the project “Collection and Documentation of Geothematic Information for Urban Areas in Greece”. Funded by Competiveness Priority Axis 7: Measure 7.3 and ERDF.

We would like to thank Dr. S. Chiotis for his contribution on the design and the materialization of the project. We also thank Dr. P. Giannoulopoulos, who provided us with borehole logs of previous studies and also with information about the hydrogeological conditions of the study area; Dr A. Koutsouveli and Mr E. Apostolidis, who supervised the drilling and the geotechnical laboratory study; and A. Fotiadis who provided us with the geological map of the study area.

Thanks are also due to Dr. K. Dimitropoulos, geophysicist in Hellenic Petroleum for his comments and to Mr. G. Michaletos, engineer of our team for his support in fieldwork.

Thanks are due to two anonymous reviewers for their constructive comments to improve the initial version of the paper.

References

Abbott, R.E., Louie, J.N., Caskey, S.J., Pullammanappallil, S., 2001. Geophysical confirmation of low-angle normal slip on the historically active Dixie Valley fault, Nevada. Journal of Geophysical Research 106 (B3), 4169–4181.

Ambraseys, N.N., Jackson, J.A., 1990. Seismicity and associated strain of central Greece between 1890 and 1988. Geophysical Journal International 101, 663–708.

Anbazhagan, P., Sitharam, T.G., Vipin, K.S., 2009. Site classification and estimation of surface level seismic hazard using geophysical data and probabilistic approach. Journal of Applied Geophysics 68 (2), 219–230.

Anderson, E.M., 1942. The Dynamics of Faulting, 1st ed. Oliver and Boyd.

Andrus, R.D., Stokoe, K.H., 1997. Liquefaction resistance based on shear wave velocity. In: Youd, T.L., Idriss, I.M. (Eds.), Proceedings of NCEER Workshop on Evaluation of Liquefaction Resistance of Soils. Tech. Rep. NCEER-97-0022. Nat. Centre for Earthquake Engrg. Res., State University of New York at Buffalo, Buffalo, pp. 89–128.

Andrus, R.D., Stokoe, K.H., 2000. Liquefaction resistance of soils from shear-wave velocity. ASCE, Journal of Geotechnical and Geoenvironmental Engineering 126 (11), 1015–1025.

Apostolidis, P., Raptakis, D., Roumelioti, Z., Pitilakis, K., 2004. Determination of S-wave velocity structure using microtremors and spac method applied in Thessaloniki (Greece). Soil Dynamics and Earthquake Engineering 24 (1), 49–67.

Benjumea, B., Hunter, J.A., Aylsworth, J.M., Pullan, S.E., 2003. Application of high-resolution seismic techniques in the evaluation of earthquake site response, Ottawa Valley, Canada. Tectonophysics 368, 193–209.

Beresnev, I.A., Atkinson, G.M., 1997. Modeling finite-fault radiation from the ωn spectrum. Bulletin. Seismological Society of America 87, 67–84.

Beresnev, I.A., Atkinson, G.M., 1998. FINSIM — a FORTRAN program for simulating stochastic acceleration time histories from finite faults. Seismological Research Letters 69, 27–32.

Bexfield, C.E., McBride, J.H., Pugin, A.J.M., Ravat, D., Biswas, S., Nelson, W.J., Larson, T.H., Sargent, S.L., Fillerup, M.A., Tingey, B.E., Wald, L., Northcott, M.L., South, J.V., Okure, M.S., Chandler, M.R., 2006. Integration of P- and SH-wave high-resolution seismic reflection and micro-gravity techniques to improve interpretation of shallow subsurface structure: New Madrid seismic zone. Tectonophysics 420, 5–21.

Boore, D.M., 2003. Simulation of ground motion using the stochastic method. Pure and Applied Geophysics 160, 635–676.

Bradford, J.H., Sawyer, D.S., Zelt, C.A., Oldow, J.S., 1998. Imaging a shallow aquifer in temperate glacial sediments using seismic reflection profiling with DMO processing. Geophysics 63, 1248–1256.

Bradford, J.H., Liberty, L.M., Lyle, M.W., Clement, W.P., Hess, S., 2006. Imaging complex structure in shallow seismic-reflection data using prestack depth migration. Geophysics 71 (6), B175–B181.

Castro, R.R., Ruız-Cruz, E., 2005. Stochastic modeling of the 30 September 1999 Mw 7.5 earthquake, Oaxaca, Mexico. Bulletin of the Seismological Society of America 95 (6), 2259–2271.

Dufaure, J.J., 1977. Néotectonique et morphogenèse dans une péninsule méditerranéenne: le Péloponnèse. Revue De Géographie Physique Et De Géologie Dynamique. 19, 27–58. (in French).

Greek Earthquake Resistant Design Code, 2000. Earthquake Planning and Protection Organisation — Association of Civil Engineers of Greece. Athens 2001. (in Greek).

Guo, N., Fagin, S., 2002. Becoming effective velocity-model builders and depth imagers, part 1 — the basics of prestack depth migration. The Leading Edge 21, 1209-1205.

Hayashi, K., Takahashi, T., 2001. High resolution seismic refraction method using surface and borehole data for site characterisation of rocks. International Journal of Rock Mechanics and Mining Sciences 38, 807–813.

Hayashi, K., Masahito, T., Neagu, C., Yasuaki, K., Katsuaki, A., Ito, Y., 2006. Seismic investigations in residential area liquefied by Mid Niigata Prefecture Earthquake. 76 Annual Meeting, SEG, Expanded Abstracts, pp. 1505–1509.

Hough, S.E., Martin, S., Bilham, R., Atkinson, G.M., 2002. The 26 January 2001 M7.6 Bhuj, India earthquake: observed and predicted ground motions. Bulletin of the Seismological Society of America 92, 2061–2079.

Idriss, I.M., Sun, J.I., 1992. SHAKE91: A Computer Program for Conduction Equivalent Linear Seismic Response Analysis of Horizontally Layered Soil Deposits. Centre for Geotechnical Modelling, University of California.

Improta, L., Bruno, P.P., 2007. Combining seismic reflection with multifold wide-aperture profiling: an effective strategy for high-resolution shallow imaging of active faults. Geophysical Research Letters 34, 20310.

Jackson, J.A., 1987. Active normal faulting and crustal extension. In: Coward, M.P., Dewey, J.F., Hancock, P.L. (Eds.), Continental Extensional Tectonics: Geological Society Special Publications, 28, pp. 3–17.

Juang, C.H., Chen, C.J., Jiang, T., 2001. Probabilistic framework for liquefaction potential by shear wave velocity. Journal of Geotechnical and Geoenvironmental Engineering 127 (8), 670–678.

Matasovic, N., 1993. Seismic response of composite horizontally-layered soil deposits. PhD Dissertation. Civil and Environmental Engineering Department, University of California.

Matasovic, N., 2006. D-MOD_2—A Computer Program for Seismic Response Analysis of Horizontally Layered Soil Deposits, Earthfill Dams, and Solid Waste Landfills. Users's Manual. GeoMotions, LLC.

Nettleton, L.L., 1939. Determination of density for reduction of gravity observations. Geophysics 4, 167–183.

Please cite this article as: Karastathis, V.K., et al., The contribution of geophysical techniques to site characterisation and liquefaction risk assessment: Case study of Nafplion City,..., J. Appl. Geophys. (2010), doi:10.1016/j.jappgeo.2010.09.003

Okada, H., 2006. Theory of efficient array observations of microtremors with special reference to the SPAC method. Exploration Geophysics 37, 73–84.
Ordonez, G., 2002. A Computer Program for the 1D Analysis of Geotechnical Earthquake Engineering Problems. Berkeley.
Papadopoulos, G.A., Lefkopoulos, G., 1993. Magnitude–distance relations for liquefaction in soil from earthquakes. Bulletin of the Seismological Society of America 83, 925–938.
Papanikolaou, D., Logos, E., Lozios, S., Sideris, Ch., 1996. Neotectonic map of Greece, "Corinthos" sheet (scale 1:100000). Earthquake Planning and Protection Organization (E.P.P.O.) edition (in Greek).
Papathanassiou, G., Pavlides, S., Christaras, B., Pitilakis, K., 2005. Liquefaction case histories and empirical relations of earthquake magnitude versus distance from the broader Aegean region. Journal of Geodynamics 40, 257–278.
Papazachos, B.C., Papazachou, C.B., 2003. The Earthquakes of Greece. Ziti Publications. (in Greek).
Park, C.B., Miller, R.D., Xia, J., 1999. Multichannel analysis of surface waves. Geophysics 64, 800–808.
Pirttijärvi, M., 2009. GRABLOX2. Gravity Interpretation and Modeling Software Based on 3-D Block Models. User's Guide to Version 2.0. University of Oulu. Department of Physics.
Roberts, J., Asten, M., 2004. Resolving a velocity inversion at the geotechnical scale using the microtremor (passive seismic) survey method. Exploration Geophysics 35, 14–18.
Roberts, J., Asten, M., 2005. Estimating the shear velocity profile of Quaternary silts using microtremor array (SPAC) measurements. Exploration Geophysics 36, 34–40.
Roumelioti, Z., Beresnev, I., 2003. Stochastic finite-fault modeling of ground motions from the 1999 Chi-Chi, Taiwan, earthquake: application to rock and soil sites with implications for nonlinear site response. Bulletin of the Seismological Society of America 93 (4), 1691–1702.
Seed, H.B., Idriss, I.M., 1971. Simplified procedure for evaluating soil liquefaction potential. Journal of Geotechnical Engineering 97 (9), 1249–1273.
Stockwell Jr., J.W., 1999. The CWP/SU: seismic Unix package. Computers and Geosciences 25 (4), 415–419.
Theodulidis, N., Kalogeras, I., Papazachos, C., Karastathis, V., Margaris, B., Papaioannou, C., Skarlatoudis, A., 2004. HEAD 1.0: a unified HEllenic accelerogram database. Seismological Research Letters 75 (1), 36–45.
Wernicke, B., 1995. Low-angle normal faults and seismicity: a review. Journal of Geophysical Research 100 (B10), 20159–20174.
Yilmaz, O., Eser, M., Berilgen, M., 2006. A case study for seismic zonation in municipal areas. The Leading Edge 25, 319–330.
Yoon, S., Rix, G.J., 2007. Evaluation of soil improvement via blasting using array-based surface wave tests. 20th Symposium on the Application of Geophysics to Environmental and Engineering Problems (SAGEEP): Environmental and Engineering Geophysical Society, Proceedings, pp. 501–508.
Youd, T.L., Noble, S.K., 1997. Liquefaction criteria based on probabilistic analyses. Proceedings of NCEER Workshop on Evaluation of Liquefaction Resistance of Soils. National Centre for Earthquake Engineering Research. Technical Report NCEER-97-0022, pp. 201–216.
Zelt, C.A., Smith, R.B., 1992. Seismic traveltime inversion for 2-D crustal velocity structure. Geophysical Journal International 108, 16–34.

Please cite this article as: Karastathis, V.K., et al., The contribution of geophysical techniques to site characterisation and liquefaction risk assessment: Case study of Nafplion City,..., J. Appl. Geophys. (2010), doi:10.1016/j.jappgeo.2010.09.003